6. TRANSFORMERS

The first representation of transformers in the EMTP was in the form of branch resistance and inductance matrices [R] and [L]. The support routine XFORMER was written to produce these matrices from the test data of single-phase two- and three-winding transformers. Stray capacitances are ignored in these representations, and they are therefore only valid up to a few kHz.

A star circuit representation for N-winding transformers (called "saturable transformer component" in the BPA EMTP) was added later, which uses matrices [R] and $[L]^{-1}$ with the alternate equation

$$[L]^{-1}\,[v] \;=\; [L]^{-1}\,[R]\,[i] \;+\; [di/dt] \tag{6.1}$$

in the transient solution. This formulation also became useful when support routines BCTRAN and TRELEG were developed for inductance and inverse inductance matrix representations of three-phase units. An attempt was made to extend the star circuit to three-phase units as well, through the addition of a zero-sequence air-return path reluctance. This model has seldom been used, however, because the zero-sequence reluctance value is difficult to obtain.

Saturation effects have been modelled by adding extra nonlinear inductance and resistance branches to the inductance or inverse inductance matrix representations, or in the case of the star circuit, with the built-in nonlinear magnetizing inductance and iron-core resistance. A nonlinear inductance with hysteresis effects (called "pseudo-nonlinear hysteretic reactor" in the BPA EMTP) has been developed as well. An accurate representation of hysteresis and eddy current effects, of skin effect in the coils, and of stray capacitance effects is still difficult at this time, and some progress in modelling these effects can be expected in the years to come.

Surprisingly, the simplest transformer representation in the form of an "ideal" transformer was the last model to be added to the EMTP in 1982, as part of a revision to allow for voltage sources between nodes.

6.1 Transformers as Part of Thevenin Equivalent Circuits

If a disturbance occurs on the high side of a step-up transformer, then the network behind that transformer, plus the transformer itself, is usually representation as a voltage source behind R-L branches. Since the transformer inductances tend to filter out the high frequencies, such a low-frequency R-L circuit appears to be reasonable.

To explain the derivation of such Thevenin equivalent circuits, the practical example of Fig. 6.1 shall be used [80], where the feeding network consists of three generators and two three-winding transformers. The transformer short-circuit reactances are $X_{HL} = 0.117$ p.u., $X_{HT} = 0.115$ p.u., $X_{LT} = 0.241$ p.u., and the generator reactance is $X"_d = 0.1385$ p.u., all based on 100

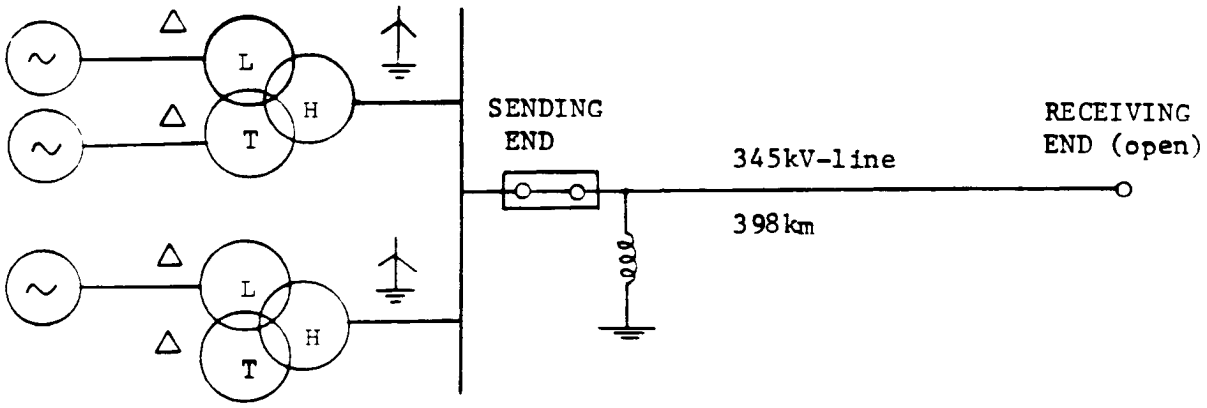

three-winding
transformers

The 4th generator was disconnected
for acceptance testing.

Fig. 6.1 - Network configuration for various field tests at CEMIG, Brazil [80]

MVA at 60 Hz. With the well-known equivalent star circuit for three-winding transformers (see Section 6.3.2), the power plant in Fig. 6.1 can be represented with the positive and zero sequence networks of Fig. 6.2. For simplicity, resistances are ignored, but they could easily be included. It is further assumed here that the zero sequence reactance values of the transformer are the same as the positive sequence values, which is only correct for three-phase banks built from single phase units, but not quite correct for three-phase units (if the zero sequence values were known,

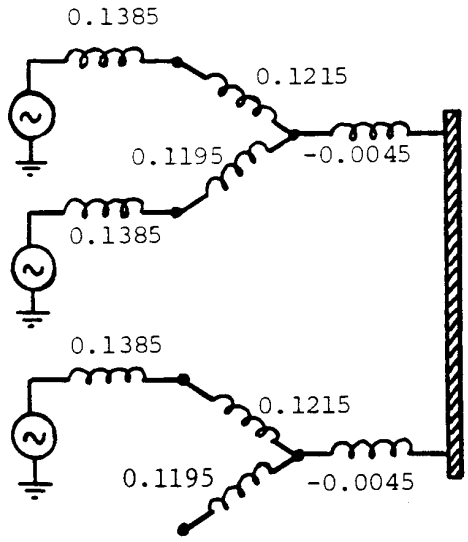

(a) Positive sequence (negative sequence identical, except that voltage sources are shorted)

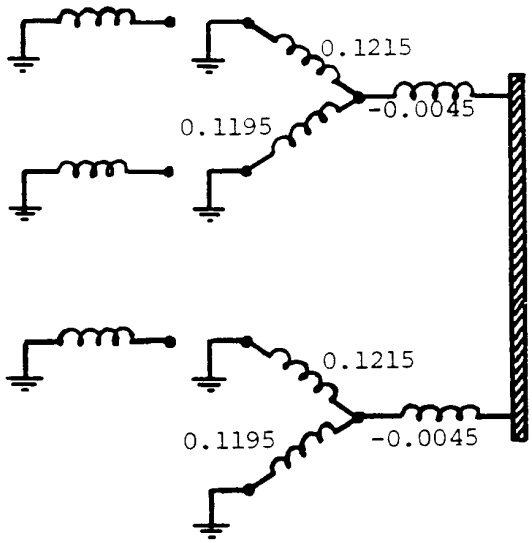

(b) Zero sequence

Fig. 6.2 - Equivalent circuits for the power plant (reactance values in p.u. based on 100 MVA at 60 Hz)

then those values could of course be used in Fig. 6.2(b)). Furthermore, the generator is modelled as a symmetrical voltage source E" behind $X"_d$. Note that the delta-connected windings act as short-circuits for zero sequence currents in Fig. 6.2(b), while the generators are disconnected to force $I_{zero} = 0$. The zero sequence parameters of the generators are therefore irrelevant in this example.

The networks of Fig. 6.2 can now be reduced to the three Thevenin equivalent circuits of Fig. 6.3, which in turn can be converted to one three-phase Thevenin equivalent circuit as shown in Fig. 6.4. This three-phase circuit is used in the EMTP for the representation of the power plant, with the data usually converted from p.u. to actual values seen from the 345 kV side ($X_{pox} = X_{neg} = 99.90\ \Omega$, $X_{zero} = 33.17\ \Omega$, or $X_s = 77.65\ \Omega$, $X_m = -22.25\ \Omega$ at 60 Hz). The symmetrical voltage sources E_a, E_b, E_c behind the coupled inductances in Fig. 6.4 are the open-circuit voltages of the power plant on the 345 kV side. In the transient simulation, the matrix [X] is obviously replaced by the inductance matrix [L].

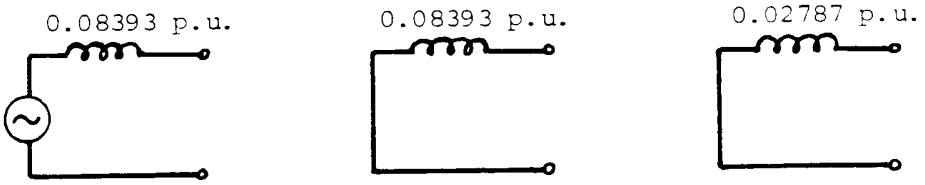

Fig. 6.3 - Thevenin equivalent circuits in sequence quantities

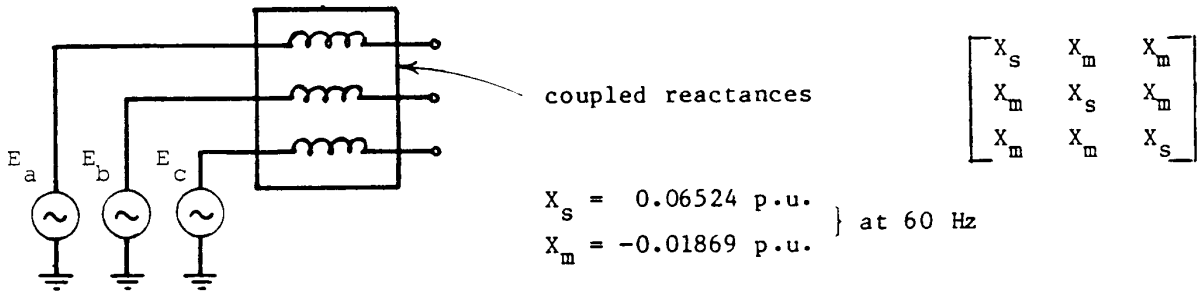

Fig. 6.4 - Three-phase Thevenin equivalent circuit in phase quantities

6.2 Inductance Matrix Representation of Single-Phase Two- and Three-Winding Transformers

Transformers can only be represented as coupled [R]-[L]-branches if the exciting current is not ignored. The derivations are fairly simple, and shall be explained with specific examples.

6.2.1 Two-Winding Transformers

Assume a short-circuit reactance of 10%, short-circuit losses of 0.5%, and an exciting current of 1%, based on the ratings V_{rating}, S_{rating} of the transformer. The excitation losses are ignored, but could be taken into account as explained in Section 6.6. If the given quantities are Z_{pu}, load losses P_{loss}, and power rating S_{rating}, then the resistance and reactance part of the short-circuit impedance are

$$R_{pu} = P_{loss} / S_{rating} \tag{6.2a}$$

$$X_{pu} = \sqrt{Z_{pu}^2 - R_{pu}^2} \tag{6.2b}$$

Since the load losses do not give any information about their distribution between windings 1 and 2, it is best to assume

$$R_{1pu} = R_{2pu} = \frac{1}{2} R_{pu} \tag{6.2c}$$

If the winding resistances are known, and not calculated from P_{loss}, then R_{1pu} and R_{2pu} may of course be different, and $R_{pu} = R_{1pu} + R_{2pu}$ is then used in Eq. (6.2b). With the T-circuit representation found in most textbooks, the p.u. impedances are then as shown in Fig. 6.5. The short-circuit impedance 0.005 + j0.10 p.u. is divided into two equal parts, and the magnetizing reactance j99.95 p.u., which is purely imaginary when excitation losses are ignored, is chosen to give an input impedance of 100 p.u. from one side, with the other side open, to make the exciting current 0.01 p.u. (the resistance 0.0025 p.u. is so small compared to 100 p.u. that it can be ignored in finding the value j99.95). The equations with the branch impedance matrix in p.u. are then

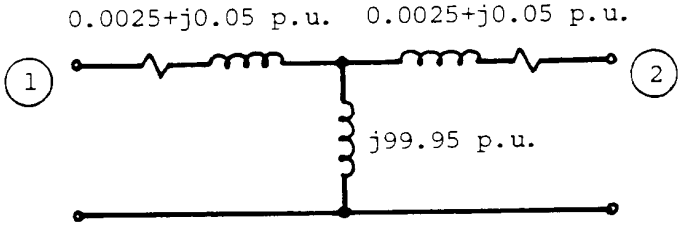

Fig. 6.5 - T-circuit representation of transformer

$$\begin{bmatrix} V_{1pu} \\ V_{2pu} \end{bmatrix} = \left[\begin{bmatrix} 0.0025 & 0 \\ 0 & 0.0025 \end{bmatrix} + j \begin{bmatrix} 100 & 99.95 \\ 99.95 & 100 \end{bmatrix} \right] \begin{bmatrix} I_{1pu} \\ I_{2pu} \end{bmatrix} \tag{6.3a}$$

for steady-state solutions, or

$$\begin{bmatrix} V_1 \\ V_2 \end{bmatrix} = [R] \begin{bmatrix} i_1 \\ i_2 \end{bmatrix} + [L] \begin{bmatrix} di_1 / dt \\ di_2 / dt \end{bmatrix} \tag{6.3b}$$

for transient solutions, with [R] being the same matrix as in Eq. (6.3a), and [L] = 1 / ω [X]. Most EMTP studies are done with actual values rather than with p.u. values. In that case, the matrix in Eq. (6.3) must be converted to actual values, with

$$[Z] = \frac{1}{S_{rating}} \left[\begin{bmatrix} 0.0025\, V_1^2 & 0 \\ 0 & 0.0025\, V_2^2 \end{bmatrix} + j \begin{bmatrix} 100\, V_1^2 & 99.95\, V_1 V_2 \\ 99.95\, V_1 V_2 & 100\, V_2^2 \end{bmatrix} \right] \Omega \qquad (6.4)$$

where S_{rating} = apparent power rating of transformer,

V_1, V_2 = voltage ratings of transformer.

Eq. (6.4) gives the [R] and [X]-matrices of coupled branches in Ω, as required by the EMTP, with the correct turns ratio V_1/V_2. If all quantities are to be referred to one side, say side 1, then simply set $V_2 = V_1$ in Eq. (6.4).

It is important to realize that the branch impedance matrix [Z] in Eq. (6.4) does not imply that the two coupled branches be connected as shown in the T-circuit of Fig. 6.5. If it were indeed limited to that connection, one could not represent a three-phase bank in wye/delta connection, because both sides would always be connected from node to ground or to some other common node. Instead, [Z] simply represents two coupled coils (Fig. 6.6). The connections are only defined through node name assignments. For example, if three single-phase transformers are connected as a three-phase bank with a grounded wye connection on side 1 and a delta connection on side 2, then the first transformer could have its two coupled branches from node HA to ground and from LA to LB, the second transformer from HB to ground and LB to LC, and the third transformer from HC to ground and LC to LA. This connection will also create the correct phase shift automatically (side 2 lagging behind side 1 by 30° for balanced positive sequence operation in this particular case).

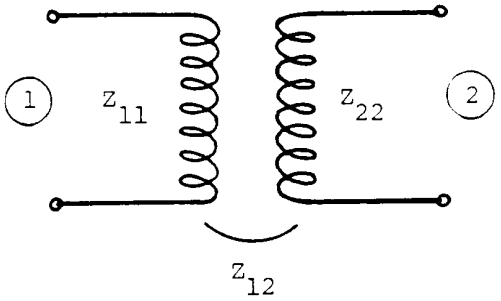

Fig. 6.6 - Two coupled coils

6.2.2 Ill-Conditioning of Inductance Matrix

The four elements in the [X]-matrix of Eq. (6.3) contain basically the information for the exciting current (magnetizing reactance X_m = 100 p.u.), with the short-circuit reactance being represented indirectly through the small differences between X_{11} and X_{12}, and between X_{22} and X_{21}. If all four values were rounded to one digit behind the decimal point ($X_{11} = X_{22} = X_{12} \approx 100$ p.u.), then the short circuit reactance would be completely lost ($X^{short} = 0$). In most studies, it is the short-circuit reactance rather than the magnetizing reactance, however, which influences the results. It is therefore important that [X] be calculated and put into the data file with very high accuracy

(typically with at least 5 or 6 digits), to make certain that the short-circuit reactance

$$X^{short} = X_{11} - \frac{X_{12}^2}{X_{22}} \quad seen\ from\ side\ 1 \tag{6.5}$$

is still reasonably accurate. It is highly recommended to calculate X^{short} from Eq. (6.5), to check how much it differs from the original test data. For a transformer with 10% short-circuit reactance and 0.4% exciting current, the values of Z_{11}, Z_{12}, Z_{22} would have to be accurate to within $\pm 0.001\%$ to achieve an accuracy of $\pm 10\%$ for X^{short}! This accuracy problem is one of the reasons why Z_{11}, Z_{12}, Z_{22} cannot be measured directly in tests if this data is to contain the short-circuit test information besides the excitation test information. Mathematically, [X] is almost singular and therefore ill-conditioned, the more so the smaller the exciting current is. Experience has shown that the inversion of [X] inside the EMTP does not cause any problems, as long as very high accuracy is used in the input data. Problems may appear on low-precision computers, however. The author therefore prefers inverse inductance matrix representations, as discussed in Section 6.3.

6.2.3 Three-Winding Transformers

The impedance matrix of single-phase three-winding transformers can be obtained in a similar way with the well-known star circuit used in Fig. 6.2. In that circuit, the magnetizing reactance is usually connected to the star point, but since its unsaturated value is much larger than the short-circuit reactances, it could be connected to either the primary, secondary or tertiary side as well. Assuming that the exciting current for the example of Fig. 6.2 is 1% measured from the primary side, with excitation losses ignored, the magnetizing reactance in the star point would then be 100.0045 p.u. Then

$$[X] = \begin{bmatrix} 100 & 100.0045 & 100.0045 \\ 100.0045 & 100.1260 & 100.0045 \\ 100.0045 & 100.0045 & 100.1240 \end{bmatrix} p.u. \tag{6.6}$$

The particular connection would again be established through the node names at both ends of the branches. For example, the three branches could be connected from node HA to ground, LA to LB, and TA to TB. To convert Eq. (6.6) to actual values, divide all elements by the power rating S_{rating}, and multiply the first row and column with voltage rating V_1, the second row and column with V_2, and the third row and column with V_3.

The [R]- and [X]-matrices can either be derived by hand, or they can be obtained from the support routines XFORMER, BCTRAN, or TRELEG in the BPA version of the EMTP. The latter two support routines were developed for three-phase units, but can be used for single-phase units as well.

6.3 Inverse Inductance Matrix Representation of Single-Phase Two- and Three-Winding Transformers

If the exciting current is ignored, then the only way to represent transformers is with matrices [R] and $[L]^{-1}$, which are handled by the EMTP as described in Section 3.4.2. The author prefers this representation over all others, because the matrices [R] and $[L]^{-1}$ are not ill-conditioned, and because any value of exciting current, including zero,

can be used. The built-in star circuit in the BPA version of the EMTP uses this representation internally as well.

For three-phase transformers, the conversion of the test data to [R]- and $[L]^{-1}$-matrices is best done with the support routine BCTRAN. For single-phase units and for three-phase transformers where $Z_{zero} \approx Z_{pos}$, the conversion is fairly simple, and can easily be done by hand, as explained next.

6.3.1 Two-Winding Transformers

First separate the short-circuit impedance into its resistance and reactance part with Eq. (6.2). The [R]- and $[\omega L]^{-1}$-matrices in p.u. can then be written down by inspection from the equivalent circuit of Fig. 6.5 (after the magnetizing inductance has been removed),

$$[R_{pu}] = \begin{bmatrix} R_{1pu} & 0 \\ 0 & R_{2pu} \end{bmatrix} \quad and \quad [\omega L_{pu}]^{-1} = \begin{bmatrix} \frac{1}{X_{pu}} & -\frac{1}{X_{pu}} \\ -\frac{1}{X_{pu}} & \frac{1}{X_{pu}} \end{bmatrix} \tag{6.7}$$

The inverse branch reactance matrix $[\omega L_{pu}]^{-1}$ is the well-known node admittance matrix of a series branch with p.u. reactance X_{pu}. For the example of Fig. 6.5, with exciting current ignored, the p.u. matrices would be

$$[R_{pu}] = \begin{bmatrix} 0.0025 & 0 \\ 0 & 0.0025 \end{bmatrix}, \qquad [\omega L_{pu}]^{-1} = \begin{bmatrix} 10 & -10 \\ -10 & 10 \end{bmatrix} \tag{6.8}$$

The matrices in Eq. (6.7) are converted to actual values with

$$[R] = \frac{1}{S_{rating}} \begin{bmatrix} R_{1pu} V_1^2 & 0 \\ 0 & R_{2pu} V_2^2 \end{bmatrix} \quad in\ \Omega \tag{6.9a}$$

$$[\omega L]^{-1} = \frac{S_{rating}}{X_{pu}} \begin{bmatrix} \frac{1}{V_1^2} & -\frac{1}{V_1 V_2} \\ -\frac{1}{V_1 V_2} & \frac{1}{V_2^2} \end{bmatrix} \quad in\ S \tag{6.9b}$$

with S_{rating} = apparent power rating

V_1, V_2 = voltage ratings.

Eq. (6.9) contains the correct turns ratio V_1/V_2. If all quantities are to be referred to one side, say side 1, then simply set $V_2 = V_1$ in Eq. (6.9). To obtain $[L]^{-1}$, the matrix in Eq. (6.9) is simply multiplied with ω.

As already mentioned in Section 3.1.2, the two coupled branches described by Eq. (6.9) can also be represented as six uncoupled branches. Ignoring the resistances for the sake of this argument, and setting

$$Y = \frac{S_{rating}}{jX_{pu}V_1^2}$$
$$t = \frac{V_1}{V_2}$$

produces the steady-state branch equations (3.3) and the alternate representations with uncoupled branches of Fig. 3.3.

6.3.2 Three-Winding Transformers

Separating R and X is more complicated now. Therefore, R shall be ignored in the following explanations. Resistances can be included, however, if the support routines BCTRAN or TRELEG are used (see Section 6.10.2 and 6.10.3). The starting point is the well-known star circuit of Fig. 6.7. Its reactances are found from the p.u. short-circuit reactances X_{HLpu}, X_{HTpu},

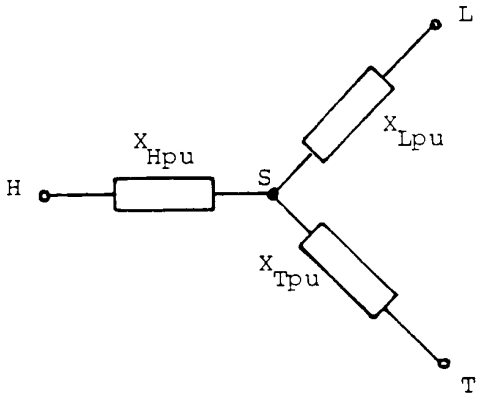

Fig. 6.7 - Star circuit for three-winding transformer with p.u. values based on voltage ratings, or with actual values referred to one side

X_{LTpu}, based on the voltage ratings and one common power base S_{base}. Since the power transfer ratings S_{HL} between H-L, S_{HT} between H-T, and S_{LT} between L-T are usually not identical, a power base conversion is usually needed. If we choose $S_{base} = 1.0$ (in same units as power ratings S_{HL}, S_{HT}, S_{LT}), then

$$\begin{aligned} X_{Hpu} &= \frac{1}{2}\left(\frac{X_{HLpu}}{X_{HL}} + \frac{X_{HTpu}}{S_{HT}} - \frac{X_{LTpu}}{S_{LT}}\right) \\ X_{Lpu} &= \frac{1}{2}\left(\frac{X_{LTpu}}{S_{LT}} + \frac{X_{HLpu}}{S_{HL}} - \frac{X_{HTpu}}{S_{HT}}\right) \\ X_{Tpu} &= \frac{1}{2}\left(\frac{X_{HTpu}}{S_{HT}} + \frac{X_{LTpu}}{S_{LT}} - \frac{X_{HLpu}}{S_{HL}}\right) \end{aligned} \qquad (6.10)$$

For the example used in Section 6.1, with $X_{HL} = 0.117$ p.u., $X_{HT} = 0.115$ p.u., $X_{LT} = 0.241$ p.u. based on 100 MVA, these star-circuit reactances based on 1 MVA would be

$$X_{Hpu} = -0.000045\,, \quad X_{Lpu} = 0.001215\,, \quad X_{Tpu} = 0.001195$$

Next, the well-known star-delta transformation is used to convert the star-circuit of Fig. 6.7 into the delta circuit of Fig. 6.8,

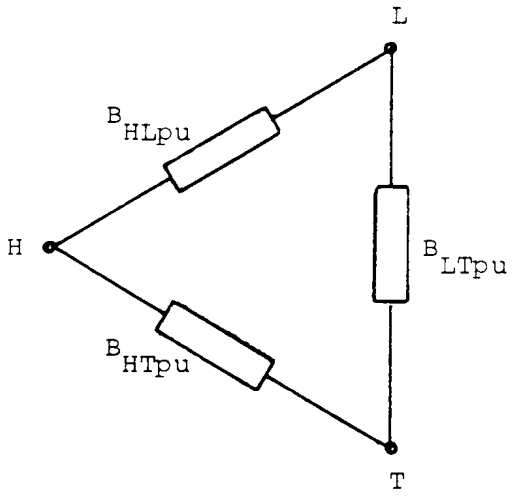

Fig. 6.9 - Delta circuit

which gives us the susceptances[1]

$$\begin{aligned} B_{HLpu} &= \frac{X_{Tpu}}{X^2} \\ B_{HTpu} &= \frac{X_{Lpu}}{X^2} \\ B_{LTpu} &= \frac{X_{Hpu}}{X^2} \end{aligned} \tag{6.11a}$$

$$\textit{with} \quad X^2 = X_{Hpu}X_{Lpu} + X_{Lpu}X_{Tpu} + X_{Hpu}X_{Tpu} \tag{6.11b}$$

For the numerical example,

$$B_{HLpu} = 889.484\,, \quad B_{HTpu} = 904.371\,, \quad B_{LTpu} = -33.495$$

Note that the susceptances in Eq. (6.11a) are not the reciprocals of the short-circuit reactances X used in Eq. (6.10). The p.u. matrix $[\omega L_{pu}]^{-1}$ based on $S_{base} = 1.0$ is easily obtained from Fig. 6.8 with the rules for nodal admittance matrices as

[1] "Susceptance" B is used here for the reciprocal of reactance X. This is not strictly correct, because susceptance is the imaginary part of an admittance (which implies B = -1/X).

$$[\omega L_{pu}]^{-1} = \begin{bmatrix} B_{HLpu} + B_{HTpu} & -B_{HLpu} & -B_{HTpu} \\ -B_{HLpu} & B_{HLpu} + B_{LTpu} & -B_{LTpu} \\ -B_{HTpu} & -B_{LTpu} & B_{HTpu} + B_{LTpu} \end{bmatrix} \tag{6.12}$$

or for the numerical example,

$$[\omega L_{pu}]^{-1} = \begin{bmatrix} 1793.855 & -889.484 & -904.371 \\ -889.484 & 855.989 & 33.495 \\ -904.371 & 33.495 & 870.876 \end{bmatrix} \quad \textit{based on 1 MVA}$$

The matrix $[\omega L_{pu}]^{-1}$ in actual values is found as

$$[\omega L]^{-1} = \begin{bmatrix} 1st \textit{ row and column of } (6.12) \textit{ multiplied with } 1/V_H \\ 2nd \textit{ row and column of } (6.12) \textit{ multiplied with } 1/V_L \\ 3rd \textit{ row and column of } (6.12) \textit{ multiplied with } 1/V_T \end{bmatrix} \textit{ in S} \tag{6.13}$$

This matrix will contain the correct turns ratios. If all quantities are to be referred to one side, say side H, then simply set $V_L = V_T = V_H$ in Eq. (6.13). Since the p.u. values are based on 1 MVA, the voltages in Eq. (6.13) must be in kV.

6.4 Matrix Representation of Single-Phase N-Coil Transformers

The newer support routines BCTRAN and TRELEG are not limited to the particular case of two or three coils, but work for any number of coils. If each winding is represented as only one coil[2], then transformers with more than three coils will seldom be encountered, but if each winding is represented as an assembly of coils, then transformer models for more than three coils are definitely needed. Breaking one winding up into an assembly of coils may well be required for yet to be developed high-frequency models with stray capacitances.

To explain the concept, only single-phase N-coil transformers are considered in this section. The extension to three-phase units is described in Section 6.5. For such an N-coil transformer, the steady-state equations with a branch impedance matrix [Z] are

[2]A coil is "an assemblage of successive convolutions of a conductor," whereas a winding is "an assembly of coils." [76] Since a winding may either be represented as one or as more coils, the more general term "coil" is used here.

$$\begin{bmatrix} V_1 \\ V_2 \\ . \\ . \\ . \\ V_N \end{bmatrix} = \begin{bmatrix} Z_{11} & Z_{12} & \dots & Z_1N \\ Z_{21} & Z_{22} & \dots & Z_2N \\ & & & \\ . & . & . & . \\ & & & \\ Z_{N1} & Z_{N2} & \dots & Z_{NN} \end{bmatrix} \begin{bmatrix} I_1 \\ I_2 \\ . \\ . \\ . \\ I_N \end{bmatrix} \tag{6.14}$$

The matrix in Eq. (6.14) is symmetric. Its elements could theoretically be measured in excitation tests: If coil k is energized, and all other coils are open-circuited, then the measured values for I_k and $V_1,\dots V_N$ produce column k of the [Z] matrix,

$$Z_{ik} = V_i / I_k \tag{6.15}$$

Unfortunately, the short-circuit impedances, which describe the more important transfer characteristics of the transformer, get lost in such excitation measurements, as mentioned in Section 6.2. It is therefore much better to use the branch admittance matrix formulation

$$[I] = [Y]\,[V] \tag{6.16}$$

which is the inverse relationship of Eq. (6.14). Even though [Z] becomes infinite for zero exciting current, or ill-conditioned for very small exciting currents, [Y] does exist, and is in fact the well-known representation of transformers used in power flow studies. Furthermore, all elements of [Y] can be obtained directly from the standard short-circuit test data, without having to use any equivalent circuits. This is especially important for N > 3, because the star-circuit "saturable transformer component" in the BPA EMTP) is incorrect for more than three coils.

For an intermediate step in obtaining [Y], the transfer characteristics between coils are needed. Let these transfer characteristics be expressed as voltage drops between coil i and the last coil N,

$$\begin{bmatrix} V_1 - V_N \\ V_2 - V_N \\ . \\ . \\ . \\ V_{N-1} - V_N \end{bmatrix} = \begin{bmatrix} Z_{11}^{reduced} & Z_{12}^{reduced} & \dots & Z_{1,N-1}^{reduced} \\ Z_{21}^{reduced} & Z_{22}^{reduced} & \dots & Z_{2,N-1}^{reduced} \\ & & & \\ . & . & . & . \\ & & & \\ Z_{N-1,1}^{reduced} & Z_{N-1,2}^{reduced} & \dots & Z_{N-1,N-1}^{reduced} \end{bmatrix} \begin{bmatrix} I_1 \\ I_2 \\ . \\ . \\ . \\ I_{N-1} \end{bmatrix} \tag{6.17}$$

with $[Z^{reduced}]$ again being symmetric. Since the exciting current has negligible influence on these transfer characteristics, it is best to ignore the exciting current altogether. Then the sum of the p.u. currents[3] (based on one common base power S_{base}, and on the transformer voltage ratings of the N coils) must be zero, or

[3]From here on it is best to work with p.u. quantities, or with quantities referred to one side, to avoid carrying the turns ratios through all the derivations.

$$\sum_{k=1}^{N} I_{k\,pu} = 0 \tag{6.18}$$

The p.u. values of the matrix elements in Eq. (6.17) can then be found directly from the short-circuit test data, as first shown by Shipley [108]. For a short-circuit test between i and N, only $I_{i\,pu}$ in Eq. (6.17) is nonzero, and $V_{N\,pu} = 0$. Then the i-th row becomes

$$V_{i\,pu} = Z_{ii\,pu}^{reduced} I_{i\,pu} \tag{6.19}$$

The impedance in this equation is the short-circuit impedance between coils i and N by definition,

$$Z_{ii\,pu}^{reduced} = Z_{iN\,pu}^{short} \tag{6.20}$$

based on one common base power S_{base}. The off-diagonal element $Z_{ik\,pu}^{reduced}$ is found by relating rows i and k of Eq. (6.17) to the short-circuit test between i and k. For this test, $I_{k\,pu} = -I_{i\,pu}$, and $V_{k\,pu} = 0$, with all other currents being zero. Then rows i and k become

$$V_{i\,pu} - V_{N\,pu} = \left(Z_{ii\,pu}^{reduced} - Z_{ik\,pu}^{reduced}\right) I_{i\,pu} \tag{6.21a}$$

$$-V_{N\,pu} = \left(Z_{ki\,pu}^{reduced} - Z_{kk\,pu}^{reduced}\right) I_{i\,pu} \tag{6.21b}$$

or after subtracting Eq. (6.21b) from (6.21a), with $Z_{ki}^{reduced} = Z_{ik}^{reduced}$,

$$V_{i\,pu} = \left(Z_{ii\,pu}^{reduced} + Z_{kk\,pu}^{reduced} - 2Z_{ik\,pu}^{reduced}\right) I_{i\,pu} \tag{6.21c}$$

By definition, the expression in parentheses of Eq. (6.21c) must be the short-circuit impedance $Z_{ik\,pu}^{short}$, or

$$Z_{ik\,pu}^{reduced} = \frac{1}{2}\left(Z_{iN\,pu}^{short} + Z_{kN\,pu}^{short} - Z_{ik\,pu}^{short}\right) \tag{6.22}$$

based on one common base power S_{base}. This completes the calculation of the matrix elements of Eq. (6.17) from the short-circuit test data, which is normally supplied by the manufacturer.

Eq. (6.17) cannot be expanded to include all coils, since all matrix elements would become infinite with the exciting current being ignored. To get to the admittance matrix formulation (6.16), Eq. (6.17) is first inverted,

$$[Y_{pu}^{reduced}] = [Z_{pu}^{reduced}]^{-1} \tag{6.23}$$

In this inverse relationship, the voltage $V_{N\,pu}$ of the last coil already exists, and all terms associated with it can be collected into a N-th column for $V_{N\,pu}$. The N-th row is created by taking the negative sum of rows 1,…N-1 based on Eq. (6.18). This results in the full matrix representation

$$\begin{bmatrix} I_{1\,pu} \\ I_{2\,pu} \\ . \\ . \\ . \\ I_{N\,pu} \end{bmatrix} = \begin{bmatrix} Y_{11\,pu} & Y_{12\,pu} & \cdots & Y_{1N\,pu} \\ Y_{21\,pu} & Y_{22\,pu} & \cdots & Y_{2N\,pu} \\ & & & \\ . & . & . & . \\ & & & \\ Y_{N1\,pu} & Y_{N2\,pu} & \cdots & Y_{NN\,pu} \end{bmatrix} \begin{bmatrix} V_{1\,pu} \\ V_{2\,pu} \\ . \\ . \\ . \\ V_{N\,pu} \end{bmatrix} \tag{6.24a}$$

with

$$Y_{ik\,pu} = Y_{ik\,pu}^{reduced} \quad \textit{from Eq. (6.23)} \quad \textit{for } i,\ k \le N-1 \tag{6.24b}$$

$$Y_{iN\,pu} = Y_{Ni\,pu} = -\sum_{k=1}^{N-1} Y_{ik\,pu}^{reduced} \quad \textit{for } i \neq N \tag{4.24c}$$

$$Y_{NN\,pu} = -\sum_{i=1}^{N-1} Y_{iN\,pu} \tag{6.24d}$$

To convert from p.u. to actual values, all elements in Eq. (6.24) are multiplied by the one common base power S_{base}, and each row and column i is multiplied with $1/V_i$.

For transient studies, the resistance and inductance parts must be separated, in a way similar to that of Section 6.3. This is best accomplished by building $[Z^{reduced}]$ only from the reactance part of the short-circuit test data, which is

$$X_{ik\,pu}^{short} = \sqrt{\left(Z_{ik\,pu}^{short}\right)^2 - \left(R_{i\,pu} + R_{k\,pu}\right)^2} \tag{6.25}$$

with $Z_{ik\,pu}^{short}$ = p.u. short circuit impedance (magnitude),

$R_{i\,pu} + R_{k\,pu}$ = either p.u. load losses in short-circuit test between i and k, or sum of p.u. winding resistances.

The winding resistances then form a diagonal matrix [R], and

$$[L]^{-1} = j\omega[Y] \tag{6.26}$$

with [Y] being purely built from reactance values jωL. Both [R] and $[L]^{-1}$ are used in Eq. (6.1) to represent the N-coil transformer.

Support routine BCTRAN uses this procedure for obtaining [R] and $[L]^{-1}$ from the transformer test data, with two additional refinements:

a. If the winding resistances are not given, but the load losses in the short-circuit tests are known, then the resistances can be calculated from Eq. (6.2) for N=2, and from the following three

equations for N = 3,

$$R_{1\,pu} + R_{2\,pu} = p_{12\,pu}^{loss}$$

$$R_{2\,pu} + R_{3\,pu} = P_{23\,pu}^{loss} \qquad (6.27)$$

$$R_{1\,pu} + R_{3\,pu} = P_{13\,pu}^{loss}$$

Strictly speaking, Eq. (6.2) and (6.27) are not quite correct, because the load losses contain stray losses in addition to the I^2R-losses, but the results should be reasonable. For transformers with 4 or more coils there is no easy way to find resistances from the load losses, and coil resistances must be specified as input data if $N \geq 4$.

b. Additional branches can be added to represent the exciting current, as described in Section 6.6.

To short derivations for a numerical example, let us first use the two-winding transformer of Fig. 6.5, with exciting current ignored. The resistance and reactance part is already separated in this case, with $R_{pu} = 0.005$ and $X_{pu} = 0.10$. The reduced reactance matrix of Eq. (6.17) is just a scalar in this case, $jX_{pu}^{reduced} = j0.10$, and its inverse is the reciprocal $Y_{pu}^{reduced} = -j10$. Adding a second row and column with Eq. (6.24) produces

$$\frac{1}{j}[\omega L_{pu}]^{-1} = \frac{1}{j}\begin{bmatrix} 10 & -10 \\ -10 & 10 \end{bmatrix}$$

which, together with $R_{1\,pu} = R_{2\,pu} = 0.0025$, is the same result shown in Eq. (6.8).

For the example of the three-winding transformer used after Eq. (6.10), the reduced reactance matrix (without the factor j) is

$$[X_{pu}^{reduced}] = \begin{bmatrix} 0.1150 & 0.1195 \\ 0.1195 & 0.2410 \end{bmatrix} \qquad based\ on\ 100\ MVA$$

which, after inversion, becomes

$$[Y_{pu}^{reduced}] = \frac{1}{j}\begin{bmatrix} 17.9386 & -8.8948 \\ -8.8948 & 8.5599 \end{bmatrix} \qquad based\ on\ 100\ MVA$$

or after adding the third row and column with Eq. (6.24),

$$[Y_{pu}] = \frac{1}{j}\begin{bmatrix} 17.93856 & -8.89484 & -9.04372 \\ -8.89484 & 8.55989 & 0.33495 \\ -9.04372 & 0.33495 & 8.70877 \end{bmatrix} \qquad based\ on\ 100\ MVA$$

which is the same answer as the one given after Eq. (6.12), except for minor round-off errors and for a change in base power from 1 MVA to 100 MVA. The star-circuit equivalent circuit of a three-winding transformer is therefore just a special case of the general method for N coils discussed here.

6.5 Matrix Representation of Three-Phase N-Coil Transformers

The first attempt to extend single-phase to three-phase transformer models was the addition of a zero-sequence reluctance to the equivalent star-circuit ("saturable transformer element" in the BPA EMTP). This was similar to the approach used on transient network analyzers, where magnetic coupling among the three core legs is usually modelled with the addition of extra delta-connected winding to a three-phase bank consisting of single-phase units. To relate the available test data to the data of the added winding is unfortunately difficult, if not impossible. For example, a two-winding three-phase unit is characterized by only two short-circuit impedances (one from the positive sequence test, and the other from the zero sequence test). Adding delta-connected windings to single-phase two-winding transformers would require three short-circuit impedances, however, because this trick converts the model into a three-winding transformer. Adding extra delta-connected windings becomes even more complicated for three-phase three-winding units, not only in fitting the model data to the test data, but also because a four-winding model would be required for which the star-circuit is no longer valid [109]. It was therefore reasonable to develop another approach, as described here.

The extension from single-phase to three-phase units turned out to be much easier than was originally thought. Conceptually, each coil of a single-phase units becomes three coils on core legs I, II, III in a three-phase unit (Fig. 6.9).

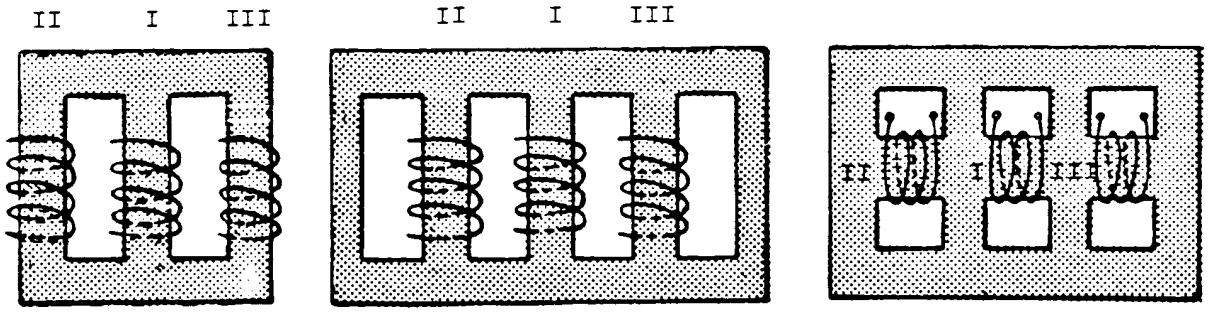

(a) Three-legged core design (b) Five-legged core design (c) Shell-type design

Fig. 6.9 - Three-phase transformers

In terms of equations, this means that each scalar quantity Z or Y must be replaced by a 3 x 3 submatrix of the form

$$\begin{bmatrix} Z_s & Z_m & Z_m \\ Z_m & Z_s & Z_m \\ Z_m & Z_m & Z_s \end{bmatrix} \tag{6.28}$$

where Z_s is the self impedance of the coil on one leg, and Z_m is the mutual impedance to the coils on the other two legs[4]. As in any other three-phase network component (e.g., overhead line), these self and mutual impedances are related to the positive and zero sequence values,

$$Z_s = \frac{1}{3}\left(Z_{zero} + 2Z_{pos}\right)$$

$$Z_m = \frac{1}{3}\left(Z_{zero} - Z_{pos}\right) \tag{6.29}$$

6.5.1 Procedure for Obtaining [R] and $[L]^{-1}$

By simply replacing scalars by 3 x 3 submatrices of the form (6.28), the [R]- and $[L]^{-1}$-matrix representation of a three-phase transformer is found as follows:

1. Set up the resistance matrix [R]. If the winding resistances are known, use them in [R]. If they are to be calculated from load losses, use Eq. (6.2) for N = 2, or Eq. (6.27) for N = 3. For N ≥ 4, there is no easy way to calculate the resistances. Use positive sequence test data in these calculations, and assume that the three corresponding coils on legs I, II, III have identical resistances.
2. Find the short-circuit reactances from Eq. (6.25) for positive sequence values. Use the same equation for zero sequence values, provided the zero sequence test between two windings does not involve another winding in delta connection. In the latter case, the data must first be modified according to Section 6.5.2.
3. Build the reduced reactance matrix $[X_{pu}^{reduced}]$ from Eq. (6.20) and (6.22), by first calculating the positive and zero sequence values separately from the positive and zero sequence short-circuit reactances, and by replacing each diagonal and off-diagonal element by a 3 x 3 submatrix of the form (6.28). The elements of this matrix are calculated with Eq. (6.29).

   Since the 3 x 3 submatrices contain only 2 distinct values X_s and X_m, it is not necessary to work with 3 x 3 matrices, but only with pairs (X_s, X_m). D. Hedman derived a "balanced-matrix algebra" for the multiplication, inversion, etc., of such "pairs" [110], which is used in the support routines BCTRAN and TRELEG.

---

[4]From Fig. 6.9 it is evident that the mutual impedance between legs I and II is slightly different from the one between legs II and III, etc. Data for this unsymmetry is usually not available, and the unsymmetry is therefore ignored here. To take it into account would require that a three-phase two-winding transformer be modelled as a six-coil transformer (Section 6.4), with 15 measured short-circuit impedances.

4. Invert $[X_{pu}^{reduced}]$ to obtain $[B_{pu}^{reduced}]$, again using Hedman's "balanced-matrix algebra," and expand $[B_{pu}^{reduced}]$ to the full matrix $[B_{pu}]$ with Eq. (6.24).

5. Since the reactances were in p.u. based on one common S_{base}, the inverse inductance matrix $[L]^{-1}$ in actual values 1/H is obtained from $[B_{pu}]$ by multiplying each element $B_{ik\ pu}$ with $\omega\ S_{base} / V_i V_k$, where V_i and V_k are the voltage ratings of coil i and k. For the conversion of p.u. resistances to actual values in Ω, multiply $R_{i\ pu}$ with V_i^2 / S_{base}.

6.5.2 Modification of Zero-Sequence Data for Delta Connections

The procedure of Section 6.5.1 cannot be used directly for the zero sequence calculation of transformers with three or more windings if one or more of them are delta-connected. Assume that a three-winding transformer has wye-connected primary and secondary windings, with their neutrals grounded, and a delta-connected tertiary winding. In this case, the zero-sequence short-circuit test between the primary and secondary windings will not only have the secondary winding shorted but the tertiary winding as well, since a closed delta connection provides a short-circuit path for zero-sequence currents. This special situation can be handled by modifying the short-circuit data for an open delta so that the procedure of Section 6.5.1 can again be used. With the well-known equivalent star circuit of Fig. 6.7, the three test values supplied by the manufacturer are ("pu" in the subscript dropped to simplify notation),

$$X_{HL}^{closed\Delta} = X_H + \frac{X_L X_T}{X_L + X_T} \tag{6.30a}$$

$$X_{HT} = X_H + X_T \qquad in\ p.u.\ values \tag{6.30b}$$

$$X_{LT} = X_L + X_T \tag{6.30c}$$

which can be solved for X_H, X_L, X_T:

$$X_H = X_{HT} - \sqrt{X_{LT} X_{HT} - X_{HL}^{closed\Delta} X_{LT}} \tag{6.31a}$$

$$X_L = X_{LT} - X_{HT} + X_H \qquad in\ p.u.\ values \tag{6.31b}$$

$$X_T = X_{HT} - X_H \tag{6.31c}$$

After this modification, the short-circuit reactances $X_H + X_L$, $X_H + X_T$ and $X_L + X_T$ are used as input data, with winding T no longer being shorted in the test between H and L.

The modification scheme becomes more complicated if resistances are included. For instance, Eq. (6.30a) becomes

$$\left| Z_{HL}^{closed\Delta} \right| = \left| R_H + jX_H + \frac{(R_L + jX_L)(R_T + jX_T)}{(R_L + R_T) + j(X_L + X_T)} \right| \qquad in\ p.u.\ values \tag{6.32}$$

with $\left|Z_{HL}^{closed\ \Delta}\right|$ being the value supplied by the manufacturer, and R_H, R_L, R_T being the winding resistances. This

leads to a system of nonlinear equations, which is solved by Newton's method in the support routine BCTRAN. It works for three-winding transformers with wye/wye/delta- and with wye/delta/delta- connections so far, which should cover most practical cases.

6.6 Exciting Current

The exciting current is very much voltage-dependent above the "knee-point" of the saturation curve $\lambda = f(i)$. Fig. 6.10 shows a typical curve for a modern high-voltage transformer with grain-oriented steel, with the knee-point around 1.1 to 1.2 times rated flux [114]. The value of the incremental inductance $d\lambda/di$ is fairly low in the saturated region, and fairly high in the unsaturated region. The exciting current in the unsaturated region can easily be included in the [L]- or $[L]^{-1}$-representations. Extra nonlinear branches are needed to include saturation effects, and extra resistance branches to include excitation losses.

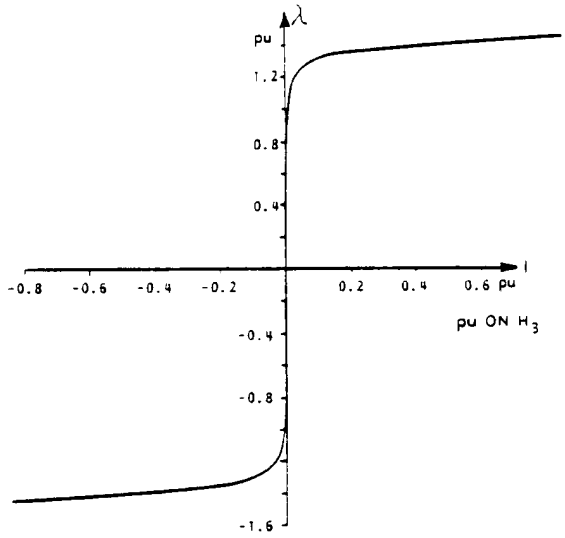

Fig. 6.10 - Typical saturation curve [114]. © 1981 IEEE

6.6.1 Linear (Unsaturated) Exciting Current

For single-phase units and for three-phase units with five-legged core or shell-type design (Fig. 6.9(b) and (c)), the linear exciting current is very small and can often be ignored. If it is ignored, then the $[L]^{-1}$-matrix representation described in Section 6.3 to 6.5 must be used. A (small) exciting current must always be included, however, if [L]-matrices are used, as explained in Section 6.2. For three-phase units with three-legged core design, the exciting current is fairly high in the zero sequence test (e.g., 100%), and should therefore not be neglected.

The exciting current has an imaginary part, which is the "magnetizing current" flowing through the magnetizing inductance L_m. It also has a smaller real part (typically 10% of the imaginary part), which accounts for excitation losses. These losses are often ignored. They can be modelled reasonably well, however, with a shunt conductance G_m in parallel with the magnetizing inductance L_m. The p.u. magnetizing conductance is

$$G_{m\,pu} = \frac{P_{exc}}{S_{rating}} \tag{6.33}$$

and the reciprocal of the p.u. magnetizing reactance is

$$\frac{1}{X_{m\,pu}} = \sqrt{\left(\frac{I_{exc}}{I_{rating}}\right)^2 - \left(G_{m\,pu}\right)^2} \tag{6.34}$$

with P_{exc} = excitation loss in excitation test,

I_{exc} = magnitude of exciting current in excitation test,

S_{rating} = power rating, and

I_{rating} = current rating.

To assess the relative magnitudes of G_m and $1/X_m$, let us take the values from the example of Section 6.2 as typical (X_{short} = 10%, R_{short} = 0.5%, I_{exc} = 1%). Furthermore, assume that the excitation loss V^2G_m at rated voltage is 25% of the load loss I^2R_{short} at rated current (a typical ratio for power transformers). Then $G_{m\,pu}$ = 0.00125 and I_{exc}/I_{rating} = 0.01. The reciprocal of the p.u. magnetizing reactance is therefore close to the value of the p.u. exciting current,

$$\frac{1}{X_{m\,pu}} \approx \frac{I_{exc}}{I_{rating}} \tag{6.35}$$

with the error being less than 1% in the numerical example.

How to include the linear exciting current in the model depends on whether an $[L]^{-1}$- or [L]-matrix representation is used, and whether the transformer is a single-phase or a three-phase unit.

6.6.1.1 Single-Phase Transformers

In the [L]-matrix representation, the magnetizing inductance L_m will already have been included in the model. Usually, the T-circuit of Fig. 6.5, or the star circuit of Fig. 6.7 with L_m connected to star point S, is used in the derivation of [L]. Since $L_{m\,pu}$ is much larger than $L_{short\,pu}$, it could be placed across the terminals of the high, low or tertiary side with equal justification. Alternatively, $2L_{m\,pu}$ could be connected to both high and low side, which would convert the T-circuit of the two-winding transformer into a π-circuit, or $3L_{m\,pu}$ could be connected to all 3 sides in the case of a three-winding transformer. The conversion of $L_{m\,pu}$ into actual values is done in the usual way by using the voltage rating for that side to which the inductance is to be connected. For example, connecting the p.u. inductance $3L_{m\,pu}$ to all 3 sides would mean that the actual values of these 3 inductances are

$$L_H = 3L_{m\,pu}\frac{V_H^{\,2}}{S_{rating}}$$

$$L_L = 3L_{m\,pu}\frac{V_L^2}{S_{rating}}$$
$$L_T = 3L_{m\,pu}\frac{V_T^2}{S_{rating}}$$

In the $[L]^{-1}$-matrix representation, the "internal" nodes of the T- or star circuit are not available, and the magnetizing inductance must therefore be connected across one or all "external" terminals, as discussed above. Connecting it across side i is the same as adding $1/L_m$ to the i-th diagonal element of $[L]^{-1}$. This makes $[L]^{-1}$ nonsingular, and it could therefore be inverted if the user prefers [R]- and [L]-matrices. This inversion option is available in the support routine BCTRAN, even though this writer prefers to work with $[L]^{-1}$ because [L] is more or less ill-conditioned as discussed in Section 6.2.2.

While L_m does not create extra branches, but "disappears" instead into the [L]- or $[L]^{-1}$-matrix, one or more extra resistance branches are needed to model excitation losses with $G_{m\,pu}$ from Eq. (6.33). Again, $G_{m\,pu}$ can either be added to one side, or 1/2 $G_{m\,pu}$ to both sides of a two-winding transformer and 1/3 $G_{m\,pu}$ to all three sides of a three-winding transformer. The conversion to actual values is again straightforward, and $R_m = 1/G_m$ is then used as input data for the extra resistance branch.

6.6.1.2 Three-Phase Transformers

The inclusion of the linear exciting current for three-phase units is basically the same as for single-phase units, except that G_m and $1/X_m$ from Eq. (6.33) and (6.34) are now calculated twice, from the positive as well as from the zero sequence excitation test data. The reciprocals of the two magnetizing inductances,

$$B_{pos} = 1/L_{m-pos}\ , \qquad B_{zero} = 1/L_{m-zero}$$

are converted to a 3 x 3 matrix

$$\begin{bmatrix} B_s & B_m & B_m \\ B_m & B_s & B_m \\ B_m & B_m & B_s \end{bmatrix}$$

where

$$B_s = \frac{1}{3}(B_{zero} + 2B_{pos})$$
$$B_m = \frac{1}{3}(B_{zero} - B_{pos}) \qquad (6.36)$$

which is added to the 3 x 3 diagonal block in $[L]^{-1}$ of the high, low, or some other side. Alternatively, 1/N-times the p.u. 3 x 3 matrix could be added to the 3 x 3 diagonal blocks of all sides of an N-winding transformer, after conversion to actual values with the proper voltage ratings. After these additions, $[L]^{-1}$ becomes nonsingular and

can therefore be inverted for users who prefer [L]-matrices. Support routine TRELEG builds an [L]-matrix directly from both the short-circuit and excitation test data, as briefly described in Section 6.10.3.

To include excitation losses, three coupled resistance branches must be added across the terminals of one side. The diagonal and off-diagonal elements of this resistance matrix are

$$R_s = \frac{1}{3}\left(\frac{1}{G_{m-zero}} + \frac{2}{G_{m-pos}}\right)$$
$$R_m = \frac{1}{3}\left(\frac{1}{G_{m-zero}} - \frac{1}{G_{m-pos}}\right) \qquad (6.37)$$

The excitation test for the positive sequence is straightforward, and the data is usually readily available. Some precautions are necessary with the zero sequence test data, if it is available, or reasonable assumptions must be made if unavailable.

If the transformer has delta-connected windings, the delta connections should be opened for the zero sequence excitation test. Otherwise, the test really becomes a short-circuit test between the excited winding and the delta-connected winding. On the other hand, if the delta is always closed in operation, any reasonable value can be used for the zero sequence exciting current (e.g., equal to positive sequence exciting current), because its influence is unlikely to show up with the delta-connected winding providing a short-circuit path for zero sequence currents.

If the zero sequence exciting current is not given by the manufacturer, a reasonable value can be found as follows: Imagine that one leg of the transformer (A in Fig. 6.11) is excited, and estimate from physical reasoning how much voltage will be induced in the corresponding coils of the other two legs (B and C in Fig. 6.11). For the three-legged core design of Fig. 6.11, approximately one half of flux λ_A returns through phases B and C, which means that the induced voltages V_B and V_C will be close to 0.5 V_A (with reversed polarity). If k is used for this factor 0.5, then

$$\frac{I_{exc-zero}}{I_{exc-pos}} = \frac{1 + k}{1 - 2k} \qquad (6.38)$$

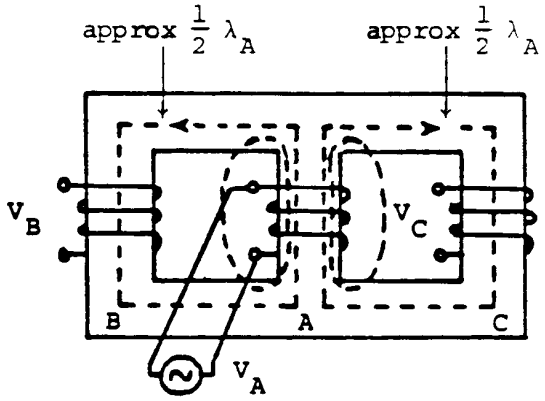

Fig. 6.11 - Fluxes in three-legged core-type design

Eq. (6.38) is derived from

$$V_A = Z_s I_A \tag{6.39a}$$

$$V_B = V_C = Z_m I_A \tag{6.39b}$$

with Z_s, Z_m being the self and mutual magnetizing impedances of the three excited coils. With

$$V_B = V_C = \frac{Z_m}{Z_s} V_A = \frac{Z_{zero} - Z_{pos}}{Z_{zero} + 2Z_{pos}} V_A = -k V_A \tag{6.40}$$

and Z_{pos}, Z_{zero} inversely proportional to $I_{exc\text{-}pos}$, $I_{exc\text{-}zero}$, Eq. (6.38) follows. Obviously, k cannot be exactly 0.5, because this would lead to an infinite zero sequence exciting current. A reasonable value for $I_{exc\text{-}zero}$ in a three-legged core design might be 100%. If $I_{exc\text{-}pos}$ were 0.5%, k would become 0.49626, which comes close to the theoretical limit of 0.5. Exciting the winding on one leg with 100 kV would then induce voltages of 49.6 kV (with reversed polarity) in the windings of the other two legs.

For the five-legged core-type design of Fig. 6.9(b), maybe 2/3 of approximately $(1/2)\lambda_A$ would return through legs B and C. In that case, k would be 1/3, or $I_{exc\text{-}zero}/I_{exc\text{-}pos} = 4$.

The excitation loss in the zero sequence test is higher than in the positive sequence test, because the fluxes λ_A, λ_B, λ_C in the three cores are now equal, and in the case of a three-legged core-type design must therefore return through air and tank, with additional eddy-current losses in the tank. Neither the value of the zero sequence exciting current nor the value of the zero sequence excitation loss are critical if the transformer has delta-connected windings, because excitation tests really become short-circuit tests in such cases.

The modification of $[L]^{-1}$ for magnetizing currents and the addition of resistance branches for excitation losses create a model which reproduces the original test data very well. Table 6.1 compares the test data, which was used to create the model with the support routine BCTRAN, with steady-state EMTP solutions in which this model was used to simulate the test conditions (e.g., voltage sources were connected to one side, and another side was shorted, to simulate a short-circuit test). In this case, the three winding resistances were specified as input data, and an [L]-matrix with 10-digit accuracy was used to minimize the problem of ill-conditioning. The excitation data was specified as being measured from the primary side, but $1/L_m$ and shunt conductance G_m were placed across the tertiary side, for reasons explained in Section 6.6.2. BCTRAN modifies L_m and R_m in this situation, to account for the influence of the short-circuit impedance between the primary and tertiary side. For the zero sequence short-circuit impedance between the primary and secondary side, the modifications of Section 6.5.2 were applied to account for the effect of the delta-connected tertiary winding.

Table 6.1 - Data for three-phase three-winding transformer in Yyd-connection

TYPE OF TEST	TEST DATA	SIMULATION RESULTS

pos. sequence excitation test	exciting current (%)	0.428	0.4281 (in phase A) 0.4280 (in phase B) 0.4230 (in phase C)
	excitation loss (kW)	135.73	135.731
zero sequence excitation test*)	exciting current (%)	0.428	0.4280 in all phases
	excitation loss (kW)	135.73	135.731
short-circuit test impedances, with three-plane MVA base in parenthesis	$\overset{pos}{Z}_{12}$ (%) (300)	8.74	8.740
	$\overset{pos}{Z}_{13}$ (%) (76)	8.68	8.680
	$\overset{pos}{Z}_{23}$ (%) (76)	5.31	5.310
	$\overset{zero}{Z}_{12}$ (%)**) (300)	7.343194***)	7.34318
	$\overset{zero}{Z}_{13}$ (%) (300)	26.258183***)	26.25806
	$\overset{zero}{Z}_{23}$ (%) (300)	18.552824***)	18.55284

*) With open delta on side 3 (values were unavailable from test; since they are unimportant if delta is closed in operation, as explained in text, the positive sequence values were used for zero sequence as well).

**) With closed delta on side 3.

***) These values were calculated from the original test data given as R and X in percent with an accuracy of 2 digits after the decimal point.

6.6.2 Saturation Effects

For the transient analysis of inrush currents, of ferroresonance and of similar phenomena it is clearly necessary to include saturation effects. Only the star circuit representation in the BPA EMTP ("saturable transformer component") accepts the saturation curve directly, while the [L]- and $[L]^{-1}$-representations require extra nonlinear inductance branches for the simulation of saturation effects.

Nonlinear inductances of the form of Fig. 6.10 can often be modelled with sufficient accuracy as two-slope piecewise linear inductances. Fig. 6.12 shows two- and five-slope piecewise linear representations from a practical case [80] for the system shown before in Fig. 6.1. The simulation results (Fig. 6.13) are almost identical, and agree reasonably well with field test results (Fig. 6.14). The slope in the saturated region above the knee is the air-core inductance, which is almost linear and fairly low compared with the slope in the unsaturated region. Typical values for air-core inductances are $2L_{short}$ (L_{short} = short-circuit inductance) for two-winding transformers with separate windings [111], or 4 to 5 times L_{short} for autotransformers. In the unsaturated region, the values can be fairly high on very large transformers (see Fig. 6.10).

While it makes little difference to which terminal the unsaturated inductance is connected,

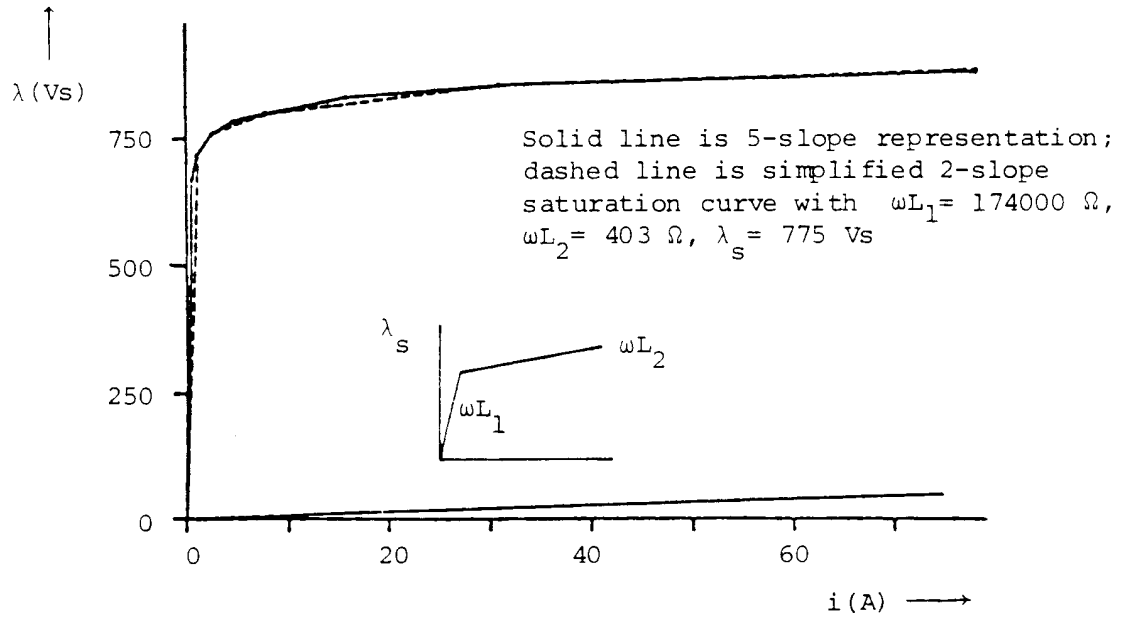

Fig. 6.12 - Two-slope and five-slope piecewise linear inductance

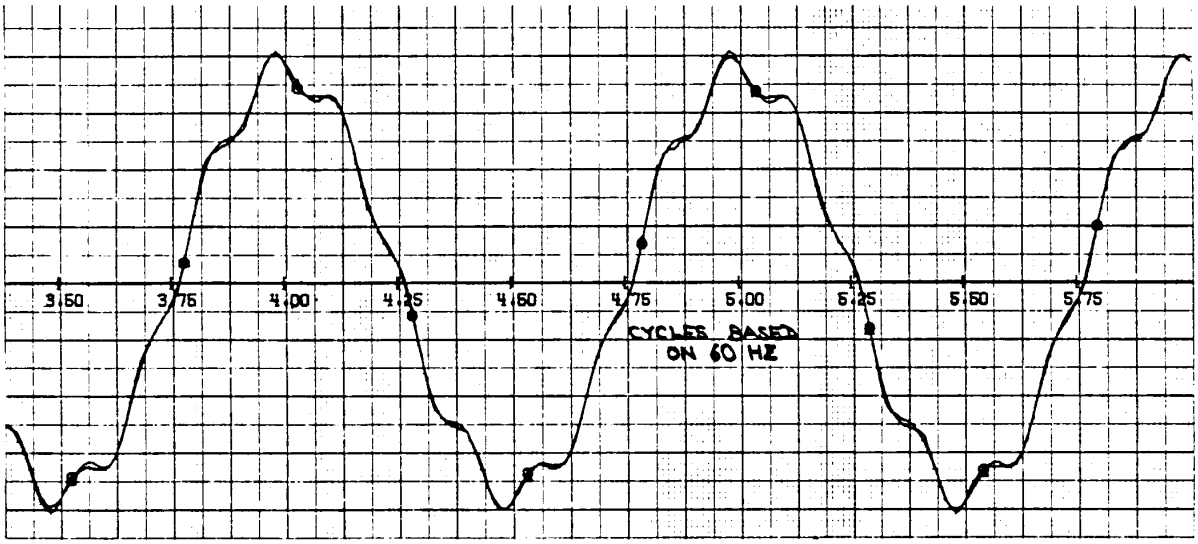

Fig. 6.13 - Superimposed EMTP simulation results with two- and five-slope piecewise linear inductance

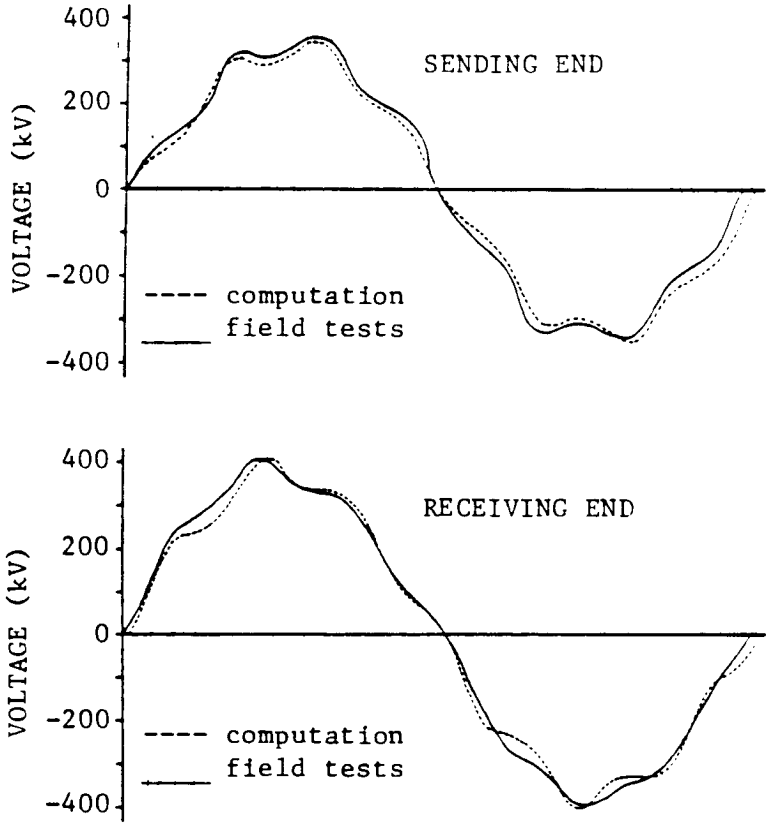

Fig. 6.14 - Comparison between simulation and field test results

it may make a difference for the saturated inductance, because of its low value. Ideally, the nonlinear inductance should be connected to a point in the equivalent circuit where the integrated voltage is equal to the iron-core flux. To identify that point is not easy, however, and requires construction details not normally available to the system analyst. For cylindrical coil construction, it can be assumed that the flux in the winding closest to the core will mostly go through the core, since there should be very little leakage. This winding is usually the tertiary winding in three-winding transformers, and in such cases it is therefore best to connect the nonlinear inductance across the tertiary terminals. Fig. 6.15 shows the star circuit derived by Schlosser [112] for a transformer with three cylindrical windings (T closest to core, H farthest from core, L in between), where the integrated voltage in point A is equal to the flux in the iron-core. The reactances of -0.58 Ω between A and T is normally not known, but it is so small compared to 7.12 Ω between S and T, that the nonlinear inductance can be connected to T instead of A, with little error. Fig. 6.15 also identifies a point B at which the integrated voltage is equal to yoke flux. Zikherman [113] suggests to connect another nonlinear inductance to that point B to represent yoke saturation. Since -4.9 Ω between H and B is small compared to 22 Ω between H and S, this second nonlinear inductance could probably be connected to H without too much error. The knee-point and the slope in the saturated region of this second nonlinear

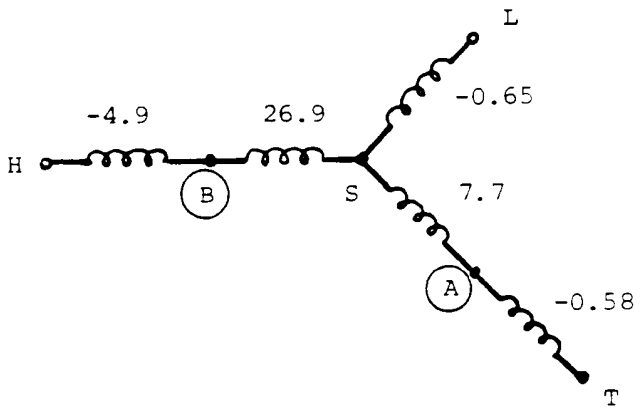

Fig. 6.15 - Reactances (in Ω) of a three-winding transformer (from [112], which provides the data for 5 cylindrical windings; the two windings farthest from the core are ignored here)

inductance are higher than those of the first nonlinear inductance (Fig. 6.16). Since it is already difficult to obtain saturation curves for the core, this secondary effect of yoke saturation is usually ignored. Dick and Watson [114] came to similar conclusions about the proper placement of the nonlinear inductance when they measured saturation curves on a three-winding transformer. Table 6.2 compares the air-core inductance (= slope in saturated region) obtained from laboratory tests with values obtained from the star circuit[5] if the nonlinear inductance is connected to the tertiary T, or to the star point S. The authors also show a more accurate equivalent circuit which would be useful if yoke saturation or unsymmetries in the three core legs are to be included. If L_m is connected to T, then the differences are less than $\pm 5\%$, whereas the differences become very large for the connection to S. Unfortunately, the built-in saturation curve in the BPA star-circuit representation ("saturable transformer component") is always connected to the star point. This model could become more useful if the code were changed so that L_m could be connected to any terminal.

[5]This star circuit also had a zero sequence inductance of 1.33 p.u. connected to the high side (see Section 6.6.2.2).

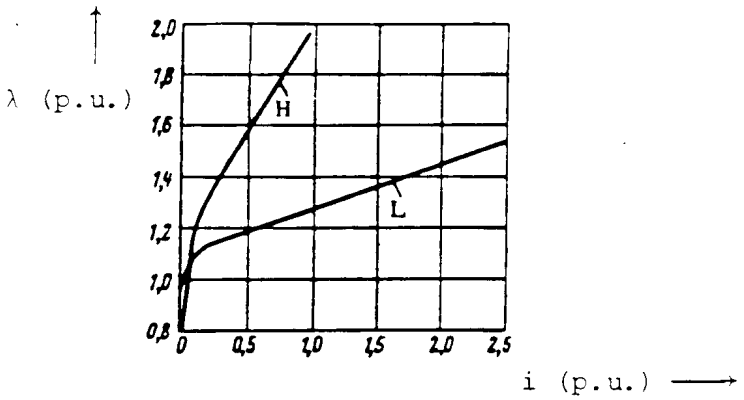

Fig. 6.16 - Nonlinear inductances connected to H (yoke saturation) and L (core saturation) of a two-winding transformer. Reprinted with permission from [113], Copyright 1972, Pergamon Journals Ltd

The proper placement of the nonlinear inductance may or may not be important, depending on the circumstances. For example, if the transformer of Table 6.2 with L_m in S were energized from the high side, then the amplitude of the inrush current would be correct. If it were energized from the tertiary side, however, then the amplitude of the inrush current would be 56% too low for high levels of saturation[6]. If details of the transformer construction are not known, then it is not easy to decide where to place L_m. In the example of Fig. 6.12-6.14, no construction details were known, and L_m was simply placed across the high voltage terminals. In spite of this, simulation results came reasonably close to field test results.

6.6.2.1 Single-Phase Transformers

If the $[L]^{-1}$-model of Section 6.3 or 6.4 is used without the corrections for linear exciting current described in Section 6.6.1, then the nonlinear inductance is simply added across the winding closest to the core. If the [L]-model of Section 6.2 is used, or if $[L]^{-1}$ has already been corrected for the linear exciting current, then a modified nonlinear inductance must be added in which the unsaturated part has been subtracted out (Fig. 6.17). This modified nonlinear inductance has an infinite slope below the knee-point.

Table 6.2 - Comparison between measured and calculated air-core inductances. © 1981 IEEE

		air-core inductance (p.u.)				
excited winding	flux measured at *)	test	calculated with L_m in T	error (%)	calculated with L_m in S	error (%)

[6]Inrush current approximately proportional to $1/L_{air\text{-}core}$ for flux above knee-point if unsaturated $L_m >> L_{air\text{-}core}$.

H	H	0.198	0.207	+4.5	0.198	0.0
	L	0.124	0.129	+4.0	0.120	-3.2
	T	0.076	0.076	0.0	0.120	+58.0
L	H	0.127	0.129	+1.6	0.120	-5.5
	L	0.131	0.125	-4.8	0.116	-11.0
	T	0.078	0.076	-2.6	0.120	+54.0
T	H	0.076	0.076	0.0	0.120	+58.0
	L	0.076	0.076	0.0	0.120	+58.0
	T	0.076	0.076	0.0	0.173	+128.0

*)Measured by integrating the voltage at that terminal. The measured short-circuit inductances were L_{HL} = 0.0738 p.u., L_{HT} = 0.1305 p.u., L_{LT} = 0.0493 p.u., which produces the star-circuit inductances of L_H = 0.0775 p.u., L_L = -0.0037 p.u., L_T = 0.0530 p.u.

6.6.2.2 Three-Phase Transformers

Usually only the positive sequence saturation curve (or the saturation curve for one core leg) is known. Then it is best to connect the same nonlinear inductance across each one of the three phases (e.g., across the tertiary terminals TA-TB, TB-TC, TC-TA). This implies that the zero sequence values are the same as the positive sequence values, which is probably a reasonable assumption for the five-legged core and shell-type construction.

For the three-legged core design, the zero sequence flux returns outside the windings through an air gap, structural steel and the tank. Fig. 6.18 shows the measured zero sequence magnetization curve for the transformer described in Table 6.2 [114]. Because of the air gap, this curve is not nearly as nonlinear as the core saturation curve of Fig. 6.10. It is therefore reasonable to approximate it as a linear magnetizing inductance. In [114] it is shown that this zero sequence magnetizing inductance should be connected to the high side. With the $[L]^{-1}$-model, this is accomplished by setting $B_{pos} = 0$ and using $B_{zero} = 1/L_{zero}$ in Eq. (6.36), and by adding the 3 x 3 matrix with $B_s = B_m = B_{zero}/3$ to the 3 x 3 diagonal block of the high side[7]. This "buries" the zero sequence magnetizing inductance in $[L]^{-1}$. The positive sequence (core leg) nonlinear inductance (Fig. 6.10 for the example taken from [114]) can then again be added across each one of the phases.

[7]By setting $B_{pos} = 0$, $[L]^{-1}$ will remain singular. This causes no problems if the inverse inductance is used. Users who prefer [L]-matrices would have to add another 3 x 3 matrix with $B_s = 2B_{pos}/3$ and $B_m = -B_{pos}/3$ to one of the sides, with $B_{pos} = 1/L_{pos}$, where L_{pos} is the linear (unsaturated) positive sequence magnetizing inductance.

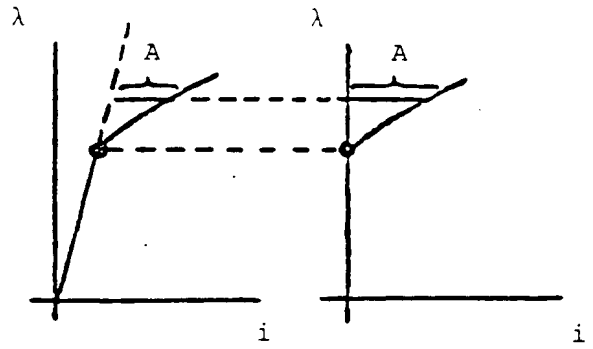

Fig. 6.17 - Subtraction of linear (unsaturated) part in saturation curve (value of A equal in both curves)

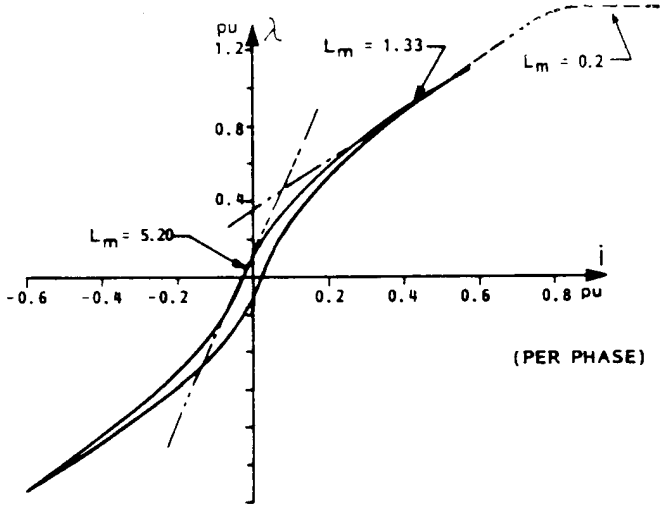

Fig. 6.18 - Zero sequence magnetization curve [114]. © 1981 IEEE

6.6.3 Hysteresis and Eddy Current Losses

The excitation losses obtained from the excitation test are mostly iron-core losses, because the I^2R-losses are comparatively small for the low values of the exciting current. These iron-core losses are sometimes ignored, but they can easily be approximated with the linear shunt conductance of G_m of Eq. (6.33).

A linear shunt conductance G_m cannot represent the iron-core losses completely accurately. These losses consist of two parts,

$$P_{iron-core} = P_{hysteresis} + P_{eddy\ current} \tag{6.41}$$

namely of hysteresis losses $P_{hysteresis}$ and of eddy current losses $P_{eddy\ current}$. In the excitation tests, these two parts cannot be separated, and only the sum $P_{iron-core}$ is obtained. Before discussing more accurate representations, it is useful to have some idea about the ratio between the two parts. Ref. [51], which may be somewhat outdated, gives ratios of

$$P_{hysteresis}/P_{eddy\ current} = 3 \qquad \textit{for silicon steel}$$

$$P_{hysteresis}/P_{eddy\ current} = 2/3 \qquad \textit{for grain-oriented steel}$$

while a more recent reference [125] quotes a typical ratio of 1/3. On modern transformers, hysteresis losses are therefore much less important than they used to be before the introduction of grain-oriented steel.

It is generally agreed that eddy current losses are proportional to λ^2 and to f^2 [51], at least in the low-frequency range, which seems to change to $f^{1.5}$ in the high-frequency range because of skin effect in the laminations. Frequency-dependent eddy current representations were discussed in [115], where R_m is replaced by a number of parallel R-L branches. It is doubtful whether this sophistication is needed, however, because the reduction caused by a proportionality change from f^2 to $f^{1.5}$ at high frequencies is probably offset by other types of loss increases (e.g., by increases in coil resistance due to skin effect, etc.). At any rate, laboratory tests would first have to be done to verify the correctness of the frequency dependence proposed in [115]. In such tests it may be difficult to separate eddy current and hysteresis losses. If we accept a proportionality with λ^2 and f^2, then a constant resistance R_m does model these losses very well, because $P_{eddy\ current} = V_{RMA}{}^2/R_m$ and $V_{RMS}{}^2 = \omega^2\lambda^2{}_{RMS}$ for sinusoidal excitation.

Hysteresis losses are a nonlinear function of flux and frequency,

$$P_{hysteresis} = k\,(\lambda)^a \cdot (f)^b \tag{6.42}$$

In [51], a is said to be close to 3 for grain-oriented steel, and b = 1. In [116], a = 2.7 and b = 1.5. If a = b = 2 were used, then the sum of hysteresis and eddy current losses could be modelled by the constant resistance R_m or conductance G_m of Eq. (6.33). This is a reasonable first approximation [125], especially if one considers that hysteresis losses are only 25% of the total iron-core losses in transformers with grain-oriented steel. Fig. 6.19(a) shows the nonlinear inductance of a current transformer, which was used by C. Taylor to duplicate field test results in a case where the secondary current was distorted by saturation effects [117]. Fig. 6.19(b) shows λ as a function of the exciting current in the transient simulation, if iron-core losses are modelled with a constant resistance R_m = 80 Ω. It can be seen that R_m not only creates the typical shape of a normal magnetization curve (with lower $d\lambda/di$ coming out of the origin, compared to $\lambda = f(i)$ in Fig. 6.19(a)), but also creates minor loops with reasonable shapes.

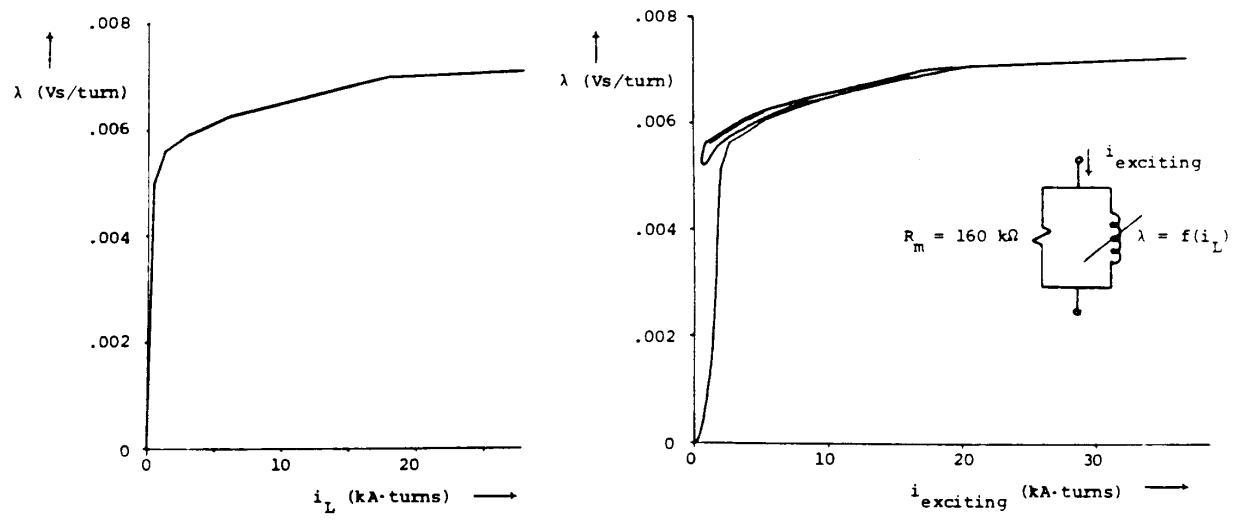

(a) Nonlinear magnetizing of current transformer

(b) Loops created by constant R_m for hysteresis and eddy current losses

Fig. 6.19 - Saturation in current transformer [117]. Reprinted by permission of C.W. Taylor

If the flux-current loop[8] for sinusoidal excitation is available, then R_m can also be calculated from

$$R_m = \frac{v}{\Delta i} \tag{6.43}$$

as an alternative to Eq. (6.33), with Δi being half of the horizontal width of the loop at $\lambda = 0$ (Fig. 6.20), and $v = \omega\lambda_{max}$. Eq. (6.43) is derived from realizing that at $\lambda = 0$ all the current must flow through the parallel resistance R_m and that the voltage reaches its peak value $\omega\lambda_{max}$ at $\lambda = 0$ because of the 90° phase shift between voltage and flux.

If more values of Δi are used at various points along the λ-axis, together with the corresponding values for $v = d\lambda/dt$, then a resistance R_m can be constructed which becomes nonlinear. This parallel combination of nonlinear resistance and nonlinear inductance has been proposed by L.O. Chua and K.A. Stromsmoe [118] to model flux-current loops caused by hysteresis and eddy current effects. They give convincing arguments why this representation is reasonable. In particular, they did make comparisons between simulations and laboratory tests, not only for a small audio output transformer with laminated silicon steel, but for a supermalloy core inductor as well. Fig. 6.21 shows the nonlinear inductances and resistances for this audio output transformer [118]. Fig. 6.22 compares the laboratory test results with simulation results [118] (first row laboratory results, second row simulation results). Fig.

[8]The author is reluctant to call it "hysteresis loop" because the losses associated with this loop are the sum of hysteresis and eddy current losses, with the latter actually being the larger part in transformers with grain-oriented steel.

6.22(a) is a family of flux-current loops for 60 Hz sinusoidal flux linkage of various amplitudes. Fig. 6.22(b) shows two loops, one with a sinusoidal flux linkage and the second with a sinusoidal current. Fig. 6.22(c) is a family of loops obtained at 60 Hz for various amplitudes of sinusoidal current. Fig. 6.22(d) shows a family of loops for sinusoidal flux linkages at 60, 120, and 180 Hz. In all cases, the agreement between measurements and simulation results is excellent. The minor loops in Fig. 6.22(e) were obtained with a 60 Hz sinusoidal current superimposed on a dc bias current. Again, there appears to be excellent agreement.

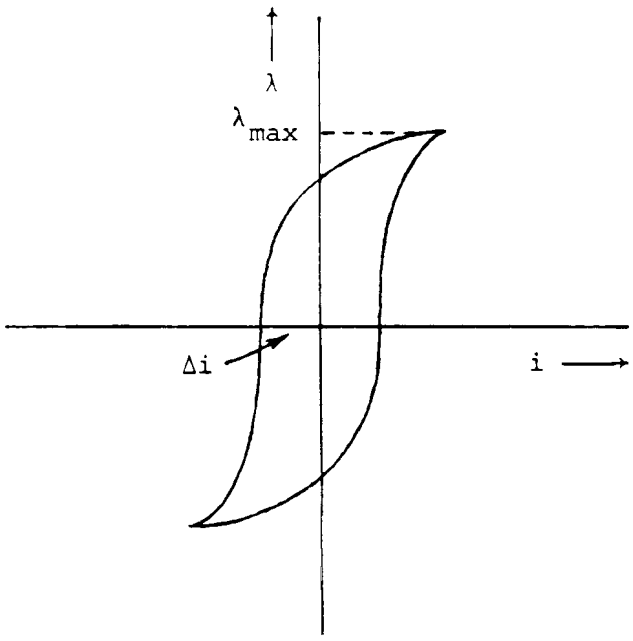

Fig. 6.20 - Flux-current loop

The major drawback of this core-loss representation with a linear or nonlinear resistance is its inability to produce the correct residual flux when the transformer is switched off. This was one of the motivations for the development of more sophisticated hysteresis models, but even these models do not seem to produce the residual flux very accurately. This writer believes that there are no models available at this time which can predict residual fluxes reliably, and that reasonable assumptions should therefore be made. There is no difficulty with the linear or nonlinear R_m-representation in starting a transient simulation with a residual flux if its value is provided as input data, as explained in Section 6.6.4.

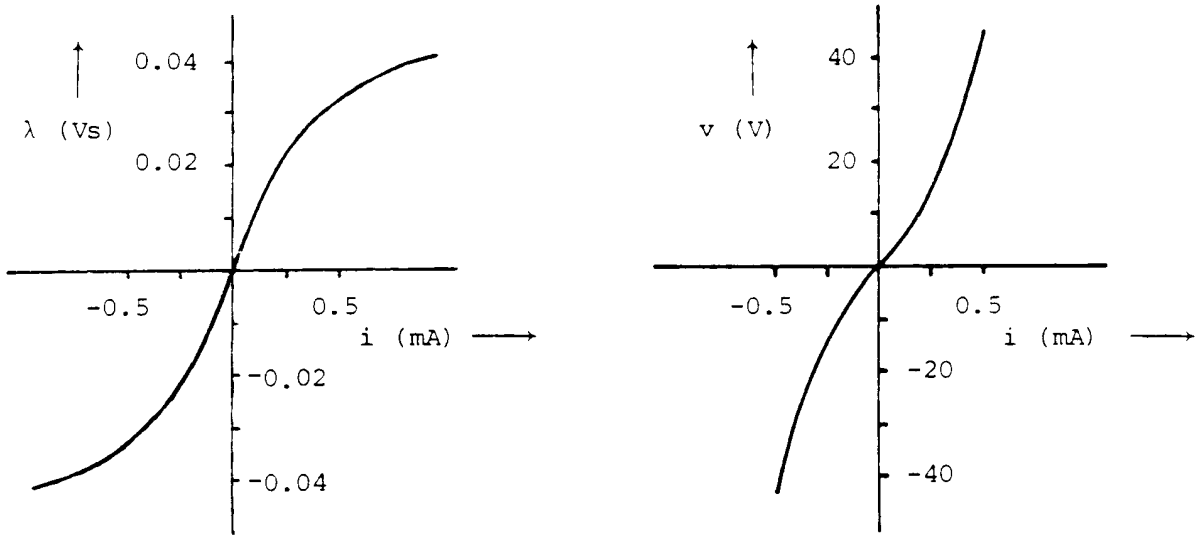

Fig. 6.21 - Model for exciting current with parallel, nonlinear resistances and inductances [118]. © 1970 IEEE

The more sophisticated models mentioned above use pre-defined trajectories or "templates" in the λ, i-plane to decide in which direction the curve will move if the flux either increases or decreases [114, 119]. The technique of [119] has been implemented in the BPA-EMTP ("pseudolinear hysteretic reactor") but a careful comparison with the simpler R_m-representations (either linear or nonlinear) has not yet been done. More research may be needed before reliable hysteresis models become available. Such models may be based on the duality between magnetic and electric circuits, which would then require the dimensions of the iron-core as input data [121], or they may be based on the physics of magnetic materials [120].

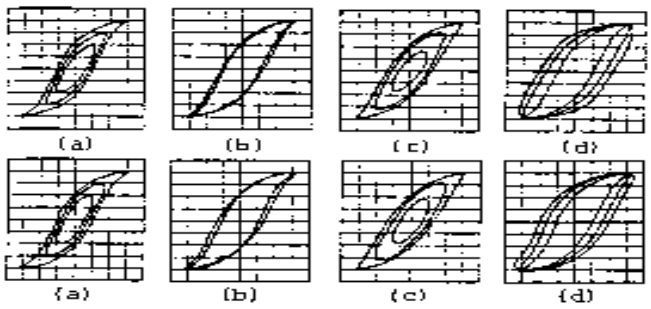

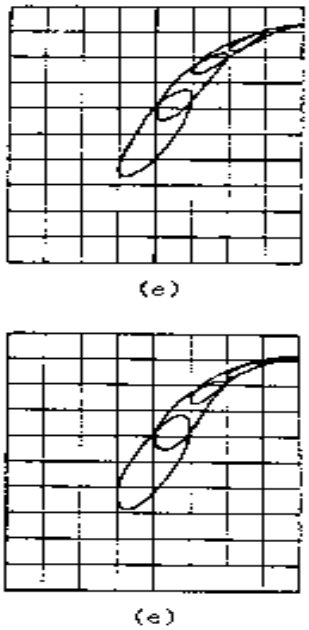

Fig. 6.22 - Comparison between measured and simulated flux-current loops [118]. © 1970 IEEE

6.6.4 Residual Flux

Residual flux is the flux which remains in the iron core after the transformer is switched off[9]. It has a major influence on the magnitude of inrush currents. Starting an EMTP simulation from a known residual flux is relatively easy, with simple as well as with sophisticated hysteresis models. To find the residual flux from a simulation is more complicated, and the results still seem to be unreliable at this time, even with sophisticated hysteresis models. Until this situation improves, it might be best to use a typical value for the residual flux as part of the input data. Unfortunately, not much data is available on residual flux. A recent survey by CIGRE [122] has not added much to it either, except for the quotation of 2 maximum values of 0.75 and 0.90 p.u. This survey does contain a reasonable amount of information about values of air-core inductances and saturation curves, however.

The UBC version of the EMTP starts the simulation from a nonzero residual flux with the following approach, in connection with piecewise linear inductances[10] (see also Section 12.1.3): At $t = 0$, the starting point A lies at $\lambda_{residual}$ and $i = 0$, and the simulation moves along a slope of L_1 (unsaturated value), as shown in Fig. 6.23. The slope is changed to L_2 (saturated value) in point B as soon as $\lambda \geq \lambda_{knee}$. At the same time, a value λ_{switch} is calculated which will bring the characteristic back through the origin when the slope is changed back to L_1 as soon as $\lambda \leq \lambda_{switch}$. Thereafter, the normal λ/i-curve will be followed. More details, in particular the problem of overshoot (λ slightly larger than λ_{knee} when going into saturation), are discussed in Section 12.1.3.3. For typical saturation curves, such as the one shown in Fig. 6.10, the linear slope is almost infinite; in that case, the first move into saturation practically lies on the given λ/i-curve, rather than somewhat higher as in Fig. 6.23.

---

[9]There seems to be some confusion in terminology between "residual" and "remanent" flux. It appears that remanent flux is the flux value at $i = 0$ in the hysteresis curve under the assumption of sinusoidal excitation.

[10]In the BPA version, this branch type has been generalized from 2 to n slopes ("pseudolinear inductor"), but it appears that is no longer accepts residual flux as input data.

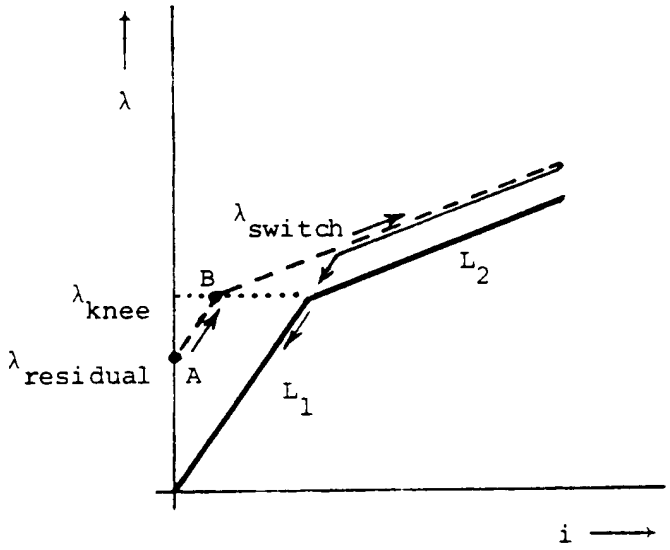

Fig. 6.23 - Starting from residual flux

The simple hysteresis model of a nonlinear L_m in parallel with a resistance R_m cannot be used to predict the residual flux after the transformer is switched off. The energy stored in L_m will simply be dissipated in R_m in this model, with an exponential decay in current and flux to zero values. The flux value at the instant of switching could possibly be close to the residual flux, but this has never been checked. Also, this value would only be meaningful if the transformer is switched off by itself, without lines or other equipment connected to it.

6.7 Autotransformers

If an autotransformer is treated the same way as a regular transformer, that is, if the details of the internal connections are ignored, the models discussed here will probably produce reasonably accurate results, except at very low frequencies. At dc, the voltage ratio between the low and high side of a full-winding transformer will be zero, whereas the voltage ratio of the autotransformer of Fig. 6.24 becomes R_{II}/R_I (dc voltage divider effect).

For a more accurate representation, series winding I and common winding II should be used as building blocks, in place of high side H and low side L. This requires a re-definition of the short-circuit data in terms of windings I and II. Since most autotransformers have a tertiary winding, this winding T shall be included in the re-definition.

First, the voltage ratings are

$$\begin{aligned} V_I &= V_H - V_L \\ V_{II} &= V_L \\ V_{III} &= V_T \end{aligned} \qquad (6.44)$$

The test between H and L provides the required data for the test between I and II directly, since II is shorted

and since the voltage applied to H is actually applied to I (b and c are at the same potential through the short-circuit connection). Only the voltage ratings are different, and the conversion from H to I is simply

$$Z_{I,II} = Z_{HL}\left(\frac{V_H}{V_H - V_L}\right)^2 \qquad in\ p.u.\ values \tag{6.45}$$

No modifications are needed for the test between II and III,

$$Z_{II,III} = Z_{LT} \qquad in\ p.u.\ values \tag{6.46}$$

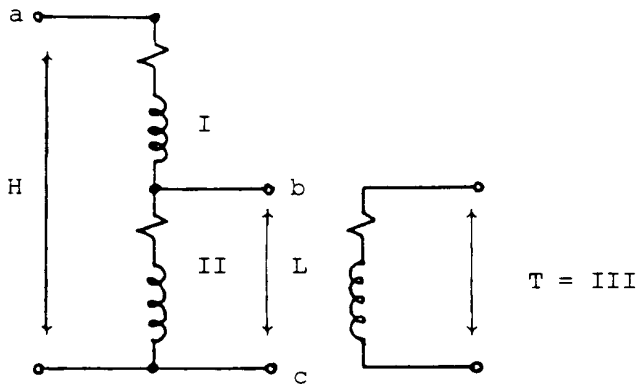

Fig. 6.24 - Autotransformer with tertiary winding

For the test between H and T, the modification can best be explained in terms of the equivalent star-circuit of Fig. 6.7, with the impedances being Z_I, Z_{II}, Z_{III}, based on V_I, V_{II}, V_{III} in this case. With III short-circuited, 1 p.u. current (based on $V_{III} = V_T$) will flow through Z_{III}. This current will also flow through I and II as 1 p.u. based on V_H, or converted to bases V_I, V_{II}, $I_I = (V_H - V_L)/V_H$ and $I_{II} = V_L/V_H$. With these currents, the p.u. voltages become

$$V_I = Z_I\frac{V_H - V_L}{V_H} + Z_{III} \qquad in\ p.u.\ values \tag{6.47}$$

$$V_{II} = Z_{II}\frac{V_L}{V_H} + Z_{III} \qquad in\ p.u.\ values \tag{6.48}$$

Converting V_I and V_{II} to physical units by multiplying Eq. (6.47) with $(V_H - V_L)$ and Eq. (6.48) with V_L, adding them, and converting the sum back to a p.u. value based on V_H produces the measured p.u. value

$$Z_{HT} = Z_I\left(\frac{V_H - V_L}{V_H}\right)^2 + Z_{II}\left(\frac{V_L}{V_H}\right)^2 + Z_{III} \qquad in\ p.u.\ values \tag{6.49}$$

Eqs. (6.45), (6.46) and (6.49) can be solved for Z_I, Z_{II}, Z_{III} since $Z_{I,II} = Z_I + Z_{II}$ and $Z_{II,III} = Z_{II} + Z_{III}$,

$$Z_{I,III} = Z_{HL}\frac{V_H V_L}{(V_H - V_L)^2} + Z_{HT}\frac{V_H}{V_H - V_L} - Z_{LT}\frac{V_L}{V_H - V_L} \quad \textit{in p.u. values} \tag{6.50}$$

The autotransformer of Fig. 6.24 can therefore be treated as a transformer with 3 windings I, II, III by simply re-defining the short-circuit impedances with Eqs. (6.45), (6.46) and (6.50). This must be done for the positive sequence tests as well as for the zero sequence tests. If the transformer has a closed delta, then the zero sequence data must be further modified as explained in Section 6.5.2, after the re-definition of the short-circuit data.

6.8 Ideal Transformer

An ideal transformer was not added to the BPA EMTP until 1982. The ideal transformer has no impedances and simply changes voltages and current from side 1 to side 2 (Fig. 6.25) as follows:

$$\frac{v_1}{v_2} = \frac{1}{n}\ ; \qquad \frac{i_1}{i_2} = n \tag{6.51}$$

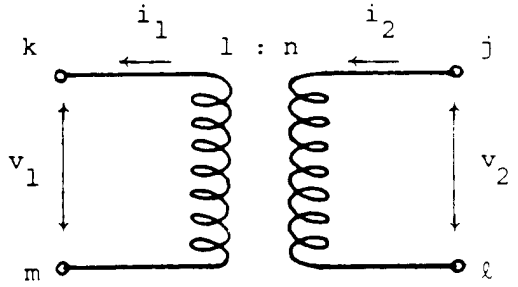

Fig. 6.25 - Ideal transformer

It is handled in the system of nodal equations (1.8a) or (1.20) by treating current i_2 as a variable, and by adding the equation

$$nv_k - nv_m - (v_j - v_\ell) = 0 \tag{6.52}$$

The matrix of the augmented system of equations, with an extra column for variable i_2, and an extra row for Eq. (6.52), then has the form of Fig. 6.26.

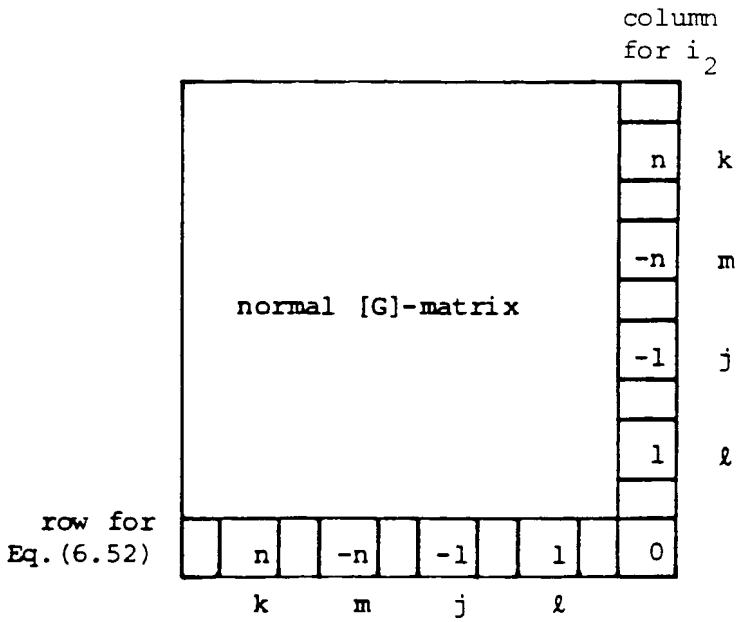

Fig. 6.26 - Augmented [G]-matrix

The ideal transformer can also be simulated with 8 resistance branches and one extra node "extra," as shown in Fig. 6.27, because these branches augment the matrix in the same way as shown in Fig. 6.26. In both approaches it is important that node "extra" (or Eq. (6.52)) is eliminated after nodes k, m, j, ℒ, to assure that the diagonal element becomes nonzero during the elimination process.

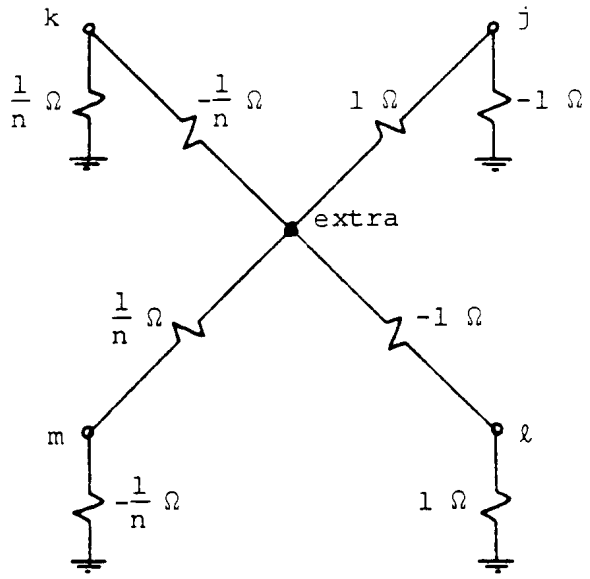

Fig. 6.27 - Resistance modelling of ideal transformer

If the transformer is unloaded ($i_2 = 0$), the elimination process will fail with a zero diagonal element. The UBC version would stop in that case with an appropriate error message, while the BPA version will first print a warning, and then continue after automatic connection of a very large resistance to the node where the zero diagonal

element has been encountered. This problem is related to the treatment of floating subnetworks (see next Section 6.9).

6.9 Floating Delta Connections

Most transmission autotransformers have delta-connected tertiary windings for the suppression of third harmonics. Frequently, nothing is connected to such tertiary windings. In that case, and in similar cases, the delta windings have floating potential with respect to ground (Fig. 6.28): only the voltages across the windings a-b, b-c, c-a are defined, but not the voltages in a, b, or c with respect to ground. Since the EMTP solves for node voltages with respect to ground, the Gauss elimination will fail with a zero diagonal element.

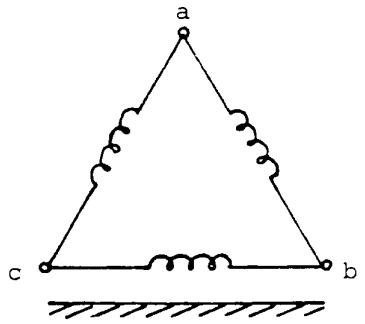

Fig. 6.28 - Floating delta connection

To prevent the solution algorithm from failing, one can either ground one of the nodes (e.g., node a), or connect stray capacitances or large shunt resistances to one or all 3 nodes. Connecting identical branches to each of the 3 nodes has the "cosmetic" advantage that the voltages in a, b, c will be symmetrical, rather than one of them being zero. The BPA version connects a large shunt resistance automatically, with an appropriate warning, whenever a zero or near-zero diagonal element is encountered. For example, if the zero diagonal is encountered at node c, then a large resistance will be connected from c to ground which will make $v_c = 0$.

6.10 Description of Support Routines and Saturable Transformer Component

Except for the "Saturable Transformer Component" in the BPA EMTP, which is an input option specifically for transformers, all other transformer representations discussed here use the general branch input option for π-circuits (with C = 0), and possibly additional linear or nonlinear, uncoupled resistance and inductance branches for the representation of the exciting current. There are three support routines XFORMER, TRELEG, and BCTRAN, which convert the transformer data into impedance or admittance matrices, as well as a support routine CONVERT for the conversion of saturation curves $V_{RMS} = f(I_{RMS})$ into $\lambda = f(i)$. These support routines, as well as the built-in saturable transformer component, are briefly described here.

6.10.1 Support Routine XFORMER

This support routine for single-phase transformers is somewhat obsolete, and has been superseded by support routine BCTRAN. For two-winding transformers, it uses essentially the approach of Section 6.3.1 to form an admittance matrix

$$[Y_{pu}] = \begin{bmatrix} \frac{1}{Z_{pu}} & -\frac{1}{Z_{pu}} \\ -\frac{1}{Z_{pu}} & \frac{1}{Z_{pu}} \end{bmatrix}$$

without first separating R and L as in Eq. (6.7). One half of $1 / jX_{m\,pu}$ from Eq. (6.35) is then added to $Y_{11\,pu}$ and $Y_{22\,pu}$, which makes the matrix nonsingular. After its inversion, and conversion from p.u. to actual values, the 2 x 2 branch impedance matrix is obtained. By not separating R and L, this impedance matrix has nonzero off-diagonal resistances, which would produce wrong results at extremely low frequencies when the magnitude of R becomes comparable with the magnitude of ωL (in one particular example, $R \approx \omega L$ at f = 0.002 Hz). At dc, an off-diagonal resistance would imply a nonzero induced voltage in the secondary winding, which should really be zero in a full-winding transformer.

For three-winding transformers, the approach of Section 6.3.2 is used. First, the impedances of the equivalent star circuit are found with Eq. (6.10), which is then converted to the delta circuit with Eq. (6.11) to obtain the 3 x 3 admittance matrix $[Y_{pu}]$ of Eq. (6.12). Again, there is no separation between R and L, and complex impedances Z are used in place of X in all these equations. One third of $1 / jX_{m\,pu}$ from Eq. (6.35) is then added to $Y_{11\,pu}$, $Y_{22\,pu}$ and $Y_{33\,pu}$, followed by matrix inversion and conversion to actual values. Again, nonzero off-diagonal resistances will appear in the branch impedance matrix, as already discussed for the two-winding transformer.

Except for errors at extremely low frequencies, which is caused by not separating R and L, the model produced by XFORMER is useful if the precautions for ill-conditioned matrices discussed in Section 6.2.2 are observed.

6.10.2 Support Routine BCTRAN

This support routine works for any number of windings, and for single-phase as well as for three-phase units. It uses the approach of Section 6.4 and 6.5 to produce the [R] and $[L]^{-1}$-matrices of coupled branches. BCTRAN has an option for inductance matrices [L] as well, in cases where the exciting current is nonzero. Because of the ill-conditioning problem (Section 6.2.2), the author prefers to work with $[L]^{-1}$ instead of [L], however.

Impedance matrices produced by BCTRAN and XFORMER differ mainly in the existence of off-diagonal resistance values in the latter case, which should make the model from BCTRAN more accurate than that from XFORMER at very low frequencies.

6.10.3 Support Routine TRELEG

This support routine was developed by V. Brandwajn at Ontario Hydro, concurrently with the development

of BCTRAN at UBC. It builds the impedance matrix (6.14) of N-winding single-phase or three-phase transformers directly from short-circuit and excitation test data, without going through the reduced impedance matrix described in Section 6.4. The exciting current must always be nonzero, and for very small values of exciting current, the matrices are subject to the ill-conditioning problem described in Section 6.2.2.

Recall that Eq. (6.14) is valid for three-phase transformers as well, if each element is replaced by 3 x 3 submatrix as discussed in Section 6.5. With this in mind, the imaginary parts of the diagonal element pairs ($X_{s\text{-}ii}$, $X_{m\text{-}ii}$) of the excited winding "i" are first calculated from the current of the positive and zero sequence excitation tests. If excitation losses are ignored, then X_{ii} in per unit is simply the reciprocal of the per-unit exciting current. With positive and zero sequence values thus known, the pair of self and mutual reactances is found from Eq. (6.29). For the other windings, it is reasonable to assume that the p.u. reactances are practically the same as for winding "i," since these open-circuit reactances are much larger than the short-circuit impedances. This will produce the imaginary parts of the other diagonal elements[11]. The real part of each diagonal element is the resistance of the particular winding.

With the diagonal element pairs known, the off-diagonal element pairs ($Z_{s\text{-}ik}$, $Z_{m\text{-}ik}$) are calculated from Eq. (6.5), except that real values X are replaced by complex values Z,

$$Z_{ik} = Z_{ki} = \sqrt{(Z_{ii} - Z_{ik}^{short})\, Z_{kk}} \tag{6.53}$$

These impedances are first calculated for positive and zero sequence, and then converted to self and mutual impedances with Eq. (6.29).

As pointed out in Section 6.2.2, the elements of [Z] must be calculated with high accuracy; otherwise, the short-circuit impedances get lost in the open-circuit impedances. The lower the exciting current is, the more equal the p.u. impedances Z_{ii}, Z_{kk} and Z_{ik} become among themselves in Eq. (6.5). Experience has shown that the positive sequence exciting current should not be much smaller than 1% for a single-precision solution on a UNIVAC computer (word length of 36 bits) to avoid numerical problems. On computers with higher precision, the value could obviously be lower. On large, modern transformers, exciting currents of less than 1% are common, but this value can usually be increased for the analysis without influencing the results. Since these ill-conditioning problems do not exist with $[L]^{-1}$, support routine BCTRAN should make TRELEG unnecessary, after careful testing of both routines has been carried out.

6.10.4 Support Routine CONVERT

Often, saturation curves supplied by manufacturers give RMS voltages as a function of RMS currents. The

[11] If it is known that the magnetizing impedance should be connected across a particular terminal, then the diagonal elements are modified to account for the differences caused by the short-circuited impedances between the terminals.

support routine CONVERT[12] changes V_{RMS}/I_{RMS}-curves into flux/current-curves $\lambda = f(i)$ with the following simplifying assumptions:

1. Hysteresis and eddy current losses in the iron-core are ignored,
2. resistance in the winding is ignored, and
3. the λ/i-curve is to be generated point by point at such distances that linear interpolation is acceptable in between points.

For the conversion it is necessary to assume that the flux varies sinusoidally at fundamental frequency as a function of time, because it is most likely that the V_{RMS}/I_{RMS}-curve has been measured with a sinusoidal terminal voltage. With assumption (2), $v = d\lambda/dt$. Therefore, the voltage will also be sinusoidal and the conversion of V_{RMS} values to flux values becomes a simple re-scaling:

$$\lambda = \frac{V_{RMS}\sqrt{2}}{\omega} \tag{6.54}$$

The re-scaling of currents is more complicated, except for point i_B at the end of the linear region A-B (Fig. 6.29):

$$i_B = I_{RMS-B}\sqrt{2} \tag{6.55}$$

The following points i_C, i_D,... are found recursively: Assume that i_E is the next value to be found. Assume further that the sinusoidal flux just reaches the value λ_E at its maximum,

$$\lambda = \lambda_E \sin \omega t \tag{6.56}$$

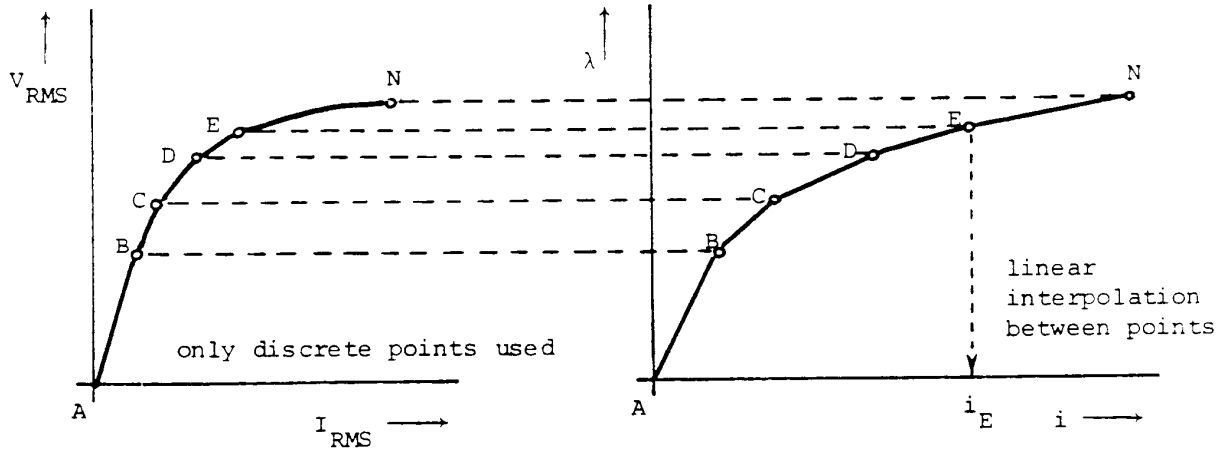

Fig. 6.29 - Recursive conversion of a V_{RMS}/I_{RMS}-curve into a λ/i-curve

Within each segment of the curve already defined by its end points, in this case A-B and B-C and C-D, i is known as a function of λ (namely piecewise linear), and with Eq. (6.56) is then also known as a function of time. Only the

[12]CONVERT was developed with the assistance of C.F. Cunha, CEMIG, Belo Horizonte, Brazil.

last segment is undefined inasmuch as i_E is still unknown. Therefore, $i = f(t,i_E)$ in the last segment. If the integral needed for RMS-values,

$$F = \frac{2}{\pi}\int_0^{\frac{\pi}{2}} i^2\, d(\omega t) \tag{6.57}$$

is evaluated segment by segment, the result will contain i_E as an unknown variable. With the trapezoidal rule of integration (reasonable step size = 1°), F has the form

$$F = a + bi_E + ci_E^2 \tag{6.58}$$

with a, b, c known. Since F must be equal to $I_{RMS\text{-}E}^2$ by definition, Eq. (6.58) can be solved for the unknown value i_E. This process is repeated recursively until the last point i_N has been found.

If the λ/i-curve thus generated is used to re-compute a V_{RMS}/I_{RMS}-curve, it will match the original V_{RMS}/I_{RMS}-curve, except for possible round-off errors. As an example, support routine CONVERT would convert the table of per-unit RMS exciting currents as a function of per-unit RMS voltages,

V_{RMS} (p.u.)	I_{RMS} (p.u.)
0	0
0.9	0.0056
1.0	0.0150
1.1	0.0401

with base power = 50 MVA and base voltage 635.1 kV, into the following flux/current relationship:

λ (Vs)	i (A)
0	0
2144.22	0.6235
2382.46	2.7238
2620.71	7.2487

This λ/i-curve is then converted back into a V_{RMS}/I_{RMS}-curve as an accuracy check. In this case, the V_{RMS} and I_{RMS} values were identical with the original input data.

Very often, the V_{RMS}/I_{RMS}-curve is only given around the knee-point, and not for high values of saturation. In such cases, it is best to do the conversion first for the given points, and then to extrapolate on the λ/i-curve with the air-core inductance.

6.10.5 Saturable Transformer Component

This built-in model was originally developed for single-phase N-winding transformers. It uses the star-circuit representation of Fig. 6.30. The primary branch with R_1, L_1 is handled as an uncoupled R-L branch between nodes $BUS1_1$, and star point S, whereas each of the other windings 2,…N is treated as a two-winding transformer (first branch from S to $BUS2_1$, second branch from $BUS1_k$ to $BUS2_k$, with k = 2,…N). The equations for each of

these two-winding transformers are derived from the cascade connection of an ideal transformer with an R-L-branch (Fig. 6.31). This leads to

$$\begin{bmatrix} di_{star}/dt \\ di_k/dt \end{bmatrix} = \frac{1}{L_k} \begin{bmatrix} \left(\frac{n_k}{n_1}\right)^2 & -\frac{n_k}{n_1} \\ -\frac{n_k}{n_1} & 1 \end{bmatrix} \begin{bmatrix} v_{star} \\ v_k \end{bmatrix} - \begin{bmatrix} \frac{R_k}{L_k} & 0 \\ 0 & \frac{R_k}{L_k} \end{bmatrix} \begin{bmatrix} i_{star} \\ i_k \end{bmatrix} \tag{6.59}$$

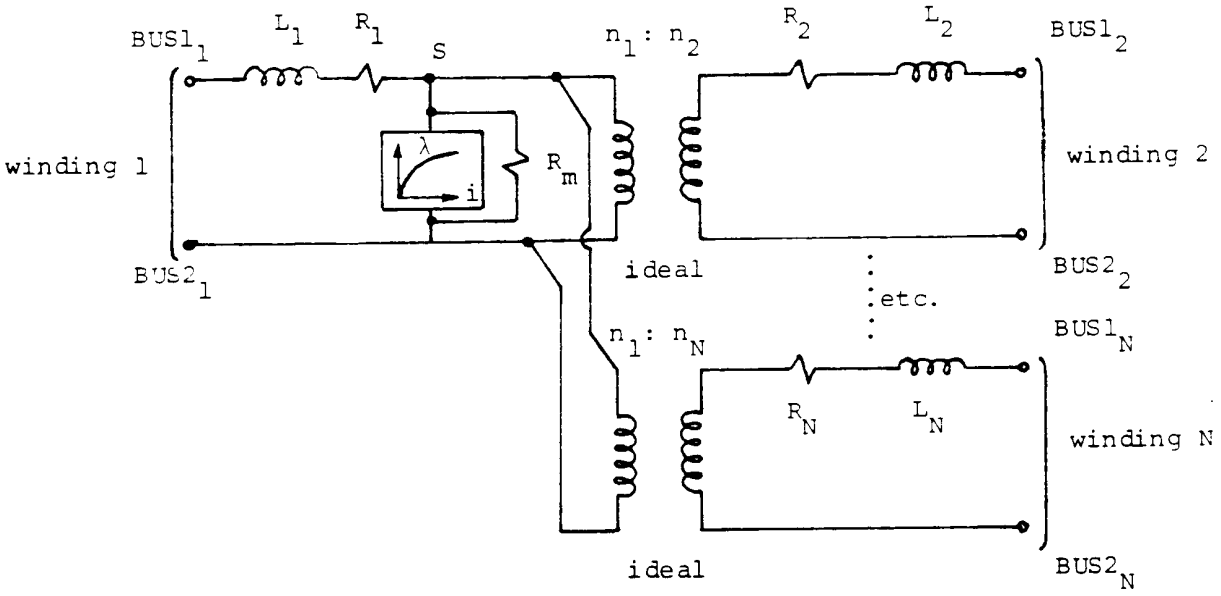

Fig. 6.30 - Star-circuit representation of N-winding transformers

Fig. 6.30 - Star-circuit representation of N-winding transformers

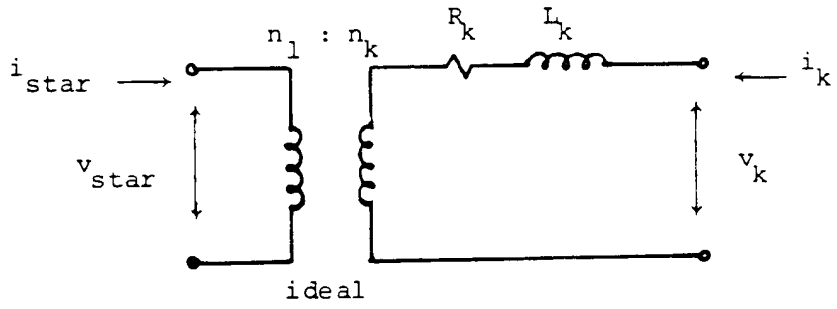

Fig. 6.31 - Cascade connection of ideal transformer and R-L-branch

which is the alternate equation (6.1) with an inverse inductance matrix $[L]^{-1}$. In the particular case of Eq. (6.59), the product $[L]^{-1}[R]$ is symmetric, which is not true in the general case.

The input data consists of the R, L-values of each star branch, and the turns ratios, as well as information for the magnetizing branch. For three-winding transformers, the impedances of the star branches are usually available in utility companies from the data files kept for short-circuit studies. If these values are in p.u., they must

be converted to actual values by using the proper voltage rating V_k for each of the star branches k = 1,…N. If the short-circuit impedances are known, then the star branch impedances can be calculated from Eq. (6.10).

The saturable transformer component has some limitations, which users should be aware of:

1. It cannot be used for more than three windings, because the star circuit is not valid for N > 3. This is more an academic than a practical limitation, because transformers with more than three windings are seldom encountered.
2. The linear or nonlinear magnetizing inductance, with R_m in parallel, is connected to the star point, which is not always the best connecting point, as explained in Section 6.6.
3. Numerical instability has occasionally been observed for the three-winding case. It is not believed to be a programming error. The source of the instability has never been clearly identified, though it is felt that it is caused by the accumulation of round-off errors. V. Brandwajn ran a case in 1985 in which the instability disappeared when the ordering of the windings was changed (e.g., first winding changed to low side from high side).
4. While the saturable transformer component has been extended from single-phase to three-phase units through the addition of a zero-sequence reluctance parameter, its usefulness for three-phase units is limited. Three-phase units are better modelled with inductance or inverse inductance matrices obtained from support routines BCTRAN or TRELEG.

6.11 Frequency-Dependent Transformer Models

At this time, no frequency-dependent effects have yet been included in the transformer model. There are basically three such effects:

a. Frequency-dependent damping in the short-circuit impedances,
b. frequency dependence in the exciting current, and
c. influence of stray capacitances at frequencies above 1 to 10 kHz.

CIGRE Working Groups [8, 18] have collected some information on the frequency-dependent L/R-ratios of short-circuit impedances (Fig. 2.17). As explained in Section 2.2.3, this frequency dependence can easily be modelled with parallel resistances, which matches the experimental curves reasonably well (Fig. 2.19). When dealing with matrices [L] or $[L]^{-1}$, resistance or conductance matrices $[R_p]$ or $[G_p]$ could be added automatically by the program, with the user simply specifying the factor k in

$$[R_p] = k\,[L] \quad , \quad or \quad [G_p] = \frac{1}{k}\,[L]^{-1} \tag{6.60}$$

Frequency-dependent effects in the exciting current were modelled with parallel R-L branches in [115], as discussed in Section 6.3.3. Whether the linear frequency dependence in these parallel R-L branches can be separated easily from the nonlinear saturation effects would have to be verified in laboratory experiments.

For transient studies which involve frequencies above a few kHz, capacitances must be added to the R-L-models. As suggested in [123], capacitances should be included

a. between the winding closest to the core, and the core,

b. between any two windings, and

c. across each winding from one end to the other.

In reality, inductances and capacitances are distributed, but reasonably accurate results, as seen from terminals, can be obtained by lumping one half of the capacitance at each end of winding for effects (a) and (b), and by lumping the total capacitance in parallel with the winding for effect (c), as shown in Fig. 6.32. Each of these capacitances can be calculated from the geometry of the transformer design. Obviously, the internal voltage distribution across a winding, which is of such great concern to the transformer design, cannot be obtained with the simple model of Fig. 6.32. Fig. 6.33 compares measured impedances of a transformer (500 MVA, 765/345/17.25 kV) and calculated impedances with a model where the capacitances were added according to Fig. 6.32. The agreement is quite good. Similar suggestions for the addition of capacitances have been made by others (e.g., [124]).

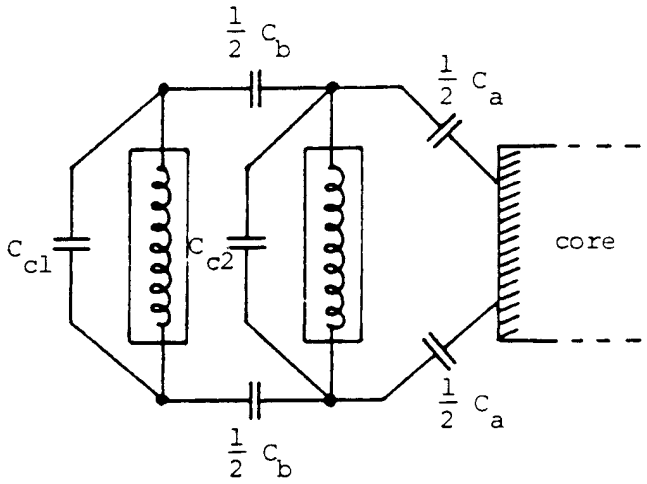

Fig. 6.32 - Addition of capacitances to R-L-model (subscripts a, b, c refer to the three effects mentioned in text)

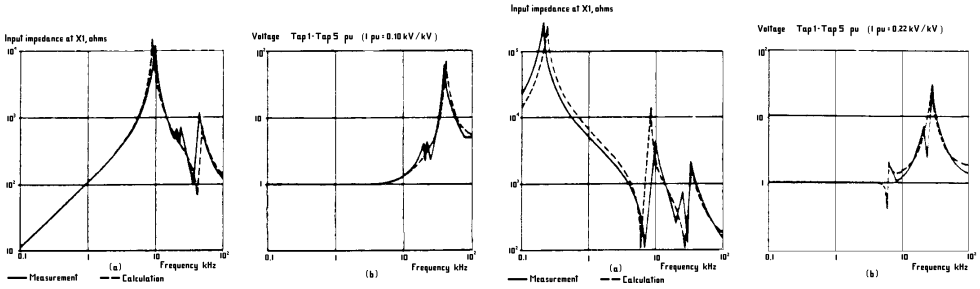

(a) X1 excited, H1, Y1, Y2 grounded

(b) X1 excited, H1, Y1, Y2 open-circuited

Fig. 6.33 - Frequency response of single-phase autotransformer with tertiary winding (marking of terminals according to North American standards: H1 = high voltage terminal, X1 = low voltage terminal, Y1, Y2 = terminals at both ends of tertiary winding) [123]. © 1981 IEEE